Energy Conversion and Management: X 18 (2023) 100376

Contents lists available at ScienceDirect

Energy Conversion and Management: X

journal homepage: www.sciencedirect.com/journal/energy-conversion-and-management-x

Dynamic performance and control strategies of micro gas turbines: State-of-the-art review, methods, and technologies

Muhammad Baqir Hashmi [a,*], Mohammad Mansouri [a,b], Mohsen Assadi [a]

[a] Department of Energy and Petroleum Engineering, University of Stavanger, 4036, Stavanger, Norway
[b] NORCE Norwegian Research Centre, 4021, Stavanger, Norway

ARTICLE INFO

Keywords:
Micro gas turbine
Cycling
Ramping
Dynamic operation
Decentralized energy systems and control strategy

ABSTRACT

The stringent energy and climate change regulations have resulted in a growing share of non-dispatchable renewable energy sources (i.e., solar and wind) in the global energy mix. This has influenced the use of fast and reliable technologies, such as micro gas turbines (MGT). The intermittency of variable renewable energy sources requires cycling, rapid load change and frequent start-ups and shutdowns of MGT. A transient phenomenon is faced during the start-up, shutdown, and load change operations. These transients may lead to several aero thermal stresses in the hot components of the gas turbines. To this end, there is a probability that the gas turbines could end up with reduced performance and safety. Therefore, the necessity for developing a critical review on dynamic performance studies of MGT becomes indispensable, to counter such adverse consequences. Variety of conventional, optimized, and artificial intelligence (AI)-based controllers adopted in the previous studies have been critically compared in the context of identification of robust controller for future applications. Apart from simple recuperated MGT cycle, the review encompassed the dynamics and control strategies of several innovative MGT cycles such as solar-based MGT, solid oxide fuel cell-based hybrid MGT, and micro humid air turbines. Digging the plethora of literature, revealed that there is a scarcity of literature pertinent to the transient performance of MGTs working on hydrogen and other alternative fuels (i.e., methanol, ammonia, syngas, and biomethane). Additionally, the paper reviews the challenges and associated solutions of alternative fuels in MGTs. The research gaps and recommendations highlighted in the present review will serve the future researchers and industry experts in assuring a reliable and safe MGT operation during transient conditions.

Introduction

Energy transition towards renewables

The tremendous global warming threat urges the decarbonization of energy systems in compliance with the UNFCCC COP-21 to prevent the global temperature rise well below 2 °C above pre-industrial levels [1,2]. The proactive solution to cap the carbon emissions lies in substituting the fossil fuel-based energy systems with renewable ones (i.e., solar, wind, biomass, etc.). In this regard, the world leaders pledged to make the world a carbon neutral zone by 2050. In line with the global measures, European Union (EU) countries devised a Climate and Energy Roadmap 2030 that emphasized on 55% reduction of greenhouse gas (GHG) emissions and 32% penetration of renewable energy sources (RES) in the energy mix by 2030 [3]. Therefore, the EU energy system is moving towards decentralization, integration, and sectoral coupling of energy systems aiming for increasing penetration of renewable energy sources. Due to the fact that solar and wind are intermittent (non-programmable) in nature, hybrid integrated systems with gas turbines are a good solution owing to operation flexibility of gas turbines [4]. In the past decades, gas turbine technology maintained a greater prestige providing decentralized, fuel flexible, environment friendly, and cost-effective energy, as compared to its counterparts (i.e., coal, and nuclear power plants). To this end, gas turbine has a promising prospect in green energy transition and future energy systems, thus, contributing to security of supply, affordability and availability of electricity and heat.

Suitability of MGT in distributed energy systems

Micro gas turbine (MGT) has emerged as a competitive energy transition technology that can withstand the increased share of renewables due to its small size, silent operation, low environmental impact, minimal maintenance, and high fuel flexibility. In addition, MGT

* Corresponding author.
E-mail address: muhammad.b.hashmi@uis.no (M. Baqir Hashmi).

https://doi.org/10.1016/j.ecmx.2023.100376
Received 11 January 2023; Received in revised form 5 March 2023; Accepted 20 March 2023
Available online 24 March 2023

Nomenclature

Abbreviations

AACPSO	Adaptive accelerated coefficient particle swarm optimization
ADRC	Active disturbance rejection control
AI	Artificial intelligence
BP	Back propagation
CCHP	Combined cooling, heating, and power
COG	Causal ordering graph
CRS	Central receiver system
CSP	Concentrated solar power
DNI	Direct normal irradiance
DDPC	Data driven predictive control
DES	Decentralized energy system
ECU	Electronic control unit
EFmGT	Externally fired micro gas turbine
ESO	Extended state observer
EU	European Union
FNNC	Fuzzy neural network control
FPID	Fuzzy proportional-integral-derivative
GA	Genetic algorithm
GHG	Greenhouse gas
GT	Gas turbine
HAT	Humid air turbine
HRB	Heat recovery boiler
H2NG	Blend of hydrogen and natural gas
HTO	High temperature orifice
ICMF	Iterative constant mass flow
ICV	Inter component volume
IGT	Industrial gas turbines
LADRC	Linear ADRC
LCOH	Levelized cost of hydrogen
LCV	Lower calorific value
LHV	Lower heating value
LVA	Lumped volume approach
MPC	Model predictive control
MGT	Micro gas turbine
mHAT	Micro humid air turbines
MV	Manipulated variables
NN	Neural network
NPV	Net present value
ODE	Ordinary differential equations
PCM	Phase change materials
PD	Proportional derivative
PEM	Polymer electrolyte membrane
PID	Proportional-integral-derivative
PMSG	Permanent magnet synchronous generator
PR	Pressure ratio
PSO	Particle swarm optimization
RBC	Rule-based control
RBF	Radial basis function
RES	Renewable energy resources
SID	Subspace identification
SM	Surge margin
SOFC	Solid oxide fuel cell
SPWM	Sinusoidal pulse width modulation
STIG	Steam injection
TES	Thermal energy storage
TIT	Turbine inlet temperature
TM	Thermal mass
TOT	Turbine outlet temperature
UHC	Unburned hydrocarbons
UNFCCC	United Nations Framework on Climate Change Convention
WI	Wobbe index

Symbols

A	Area (m^2)
a	Ambient
c	Specific heat of recuperator metal (kJ/kgK)
d	Wall thickness (m)
d	Design point
D	Characteristics diameter
e	Internal energy per unit mass
e_y	Output error
F	Force ($kgms^{-2}$)
F	Force vector
G	Torque (Nm)
g	Acceleration (m/s^2)
Gr	The Grashof number
H	Total enthalpy (kJ/kg)
h	Enthalpy (kJ/kg)
I	Shaft moment of inertia (kgm^2)
J	Quadratic cost function
k	Specific heat ratio
L	Component length (m)
$\dot{m}$	mass flow rate (kg/s)
m	Mass (kg)
$\dot{m}_a$	Ambient air mass flow rate (kg/s)
n	Surface normal unit vector
n_x	Number of heat exchanger segments
Nu	The Nusselt number
$\dot{Q}$	Heat transfer rate (kgm^2s^{-3})
r	Radius of the thermal mass (m)
t	Time (s)
$\overline{T}$	Average temperature (K)
u	Axial velocity (m/s)
u	Velocity vector
V	Infinitesimal volume of constituent components (m^3)
$\dot{W}_p$	Pressure work (kW)
$\dot{W}_s$	Shaft power (kW)
$\dot{W}_{ld}$	Load (kW)
x	Input signal of tracking differentiator
y	Output signal of tracking differentiator

Greek letters

ρ	Density (kg/m^3)
τ	Time constant
α	Convective heat transfer coefficient (kW/m^2K)
λ	Thermal conductivity ($W/(m.K)$)
β	Coefficient of thermal expansion (K^{-1})
μ	Dynamic viscosity ($Pa.s$)
ν	Kinematic viscosity (m^2s^{-1})
ω	Rotating speed (rad/s)
γ	Variable factor coefficient
η	Efficiency
∂	Partial change
Δ	difference

Subscripts

0	Reference value
c	Cold side
$comb$	Combustor
$comp$	Compressor
$cond$	Conduction
$conv$	Convection
f	fuel
h	Hot side
HX	Heat exchanger
i	control volume index

in	inlet	s	Isentropic
l	Heat exchanger segment index	*turb*	Turbine
out	Outlet		

associated with recuperator and heat recovery unit in combined heat and power (CHP) mode gives enhanced electrical efficiency and improved fuel utilization. The pursuit of enhanced energy efficiency, stability, security, and sustainability needs the MGT to be integrated with wind turbines, solar photovoltaic (PV) panels, storage devices, fuel cells, and biomass plants for decentralized applications. Moreover, another competitive advantage of MGT over its contemporary devices is the flexibility of burning various fuels such as natural gas, ethanol, dimethyl ester, diesel, hydrogen, and biomass-derived products (e.g., landfill gas, and syngas) [3].

Vulnerability to rapid and frequent ramping with renewables

The MGTs can face dynamic operation because of different reasons. Start-ups, shutdowns, load changes, and ambient conditions variations result in dynamic operation. A grid connected MGT is also subject to dynamic operation due to sudden load variations, as demanded by the grid. In addition, different integration and hybridization scenarios can result in dynamic operation. For example, integration of MGT with non-dispatchable RES, urge MGT to provide operational flexibility in terms of fast and frequent ramping in the period of unavailability of the renewables. In this regard, a quicker response is needed during frequent start-up and shutdown to meet the consumer demand. A renewable fuel based MGT in a distributed energy network is shown in Fig. 1. Although MGT has got a proven operation flexibility due to smaller size, the presence of larger volumes such as recuperator, combustor, heat recovery unit lead to a delayed dynamic response during external disturbance. The potentially delayed response is due to the metal matrix thermal inertia. These transients have a propensity of low cycle fatigue in the hot gas path components, leading to component damage and unplanned shutdown of MGT [5]. Therefore, a dynamic performance study of MGT is of paramount importance to comprehend various factors associated with sharp transients.

In the wake of above-mentioned factors urging for green energy transition, and higher penetration of RES in energy systems, MGT is one of the promising technologies. However, MGT could potentially be vulnerable to frequent and sudden load variations due to e.g., integration with RES. The consequence might be the increasing risk for failures including creep and thermal fatigue damages. Therefore, it is important to consider the effect of dynamic operations on the lifing of the MGT. In this context, an in-depth literature survey that could encompass all the information pertinent to dynamic operations of different MGTs along with modeling approaches to estimate the dynamic performance and operation control is of crucial need for further research and development. To authors' best knowledge there is no such a comprehensive review article that could combine the existing knowledge relevant to dynamic performance and operation of MGT and provide a critical analysis in this regard. Therefore, the present paper reviews the state-of-the-art in the context of dynamic performance and control studies pertinent to MGT in CHP and RES-integrated operations. The challenges of alternative fuels and dynamics related to that have also been considered. The review encompasses different numerical modeling methodologies existing in the previous literature. The significance of overlooked areas such as heat transfer effects and volume dynamics have been elaborated. Moreover, various classical and advanced control strategies have been reviewed. The research gaps and challenges presented by this review will assist the research and development in design optimization, control strategy design, fault detection and diagnostics, and condition-based maintenance of MGTs during dynamic operations contributing to enhanced performance and reliability of the technology.

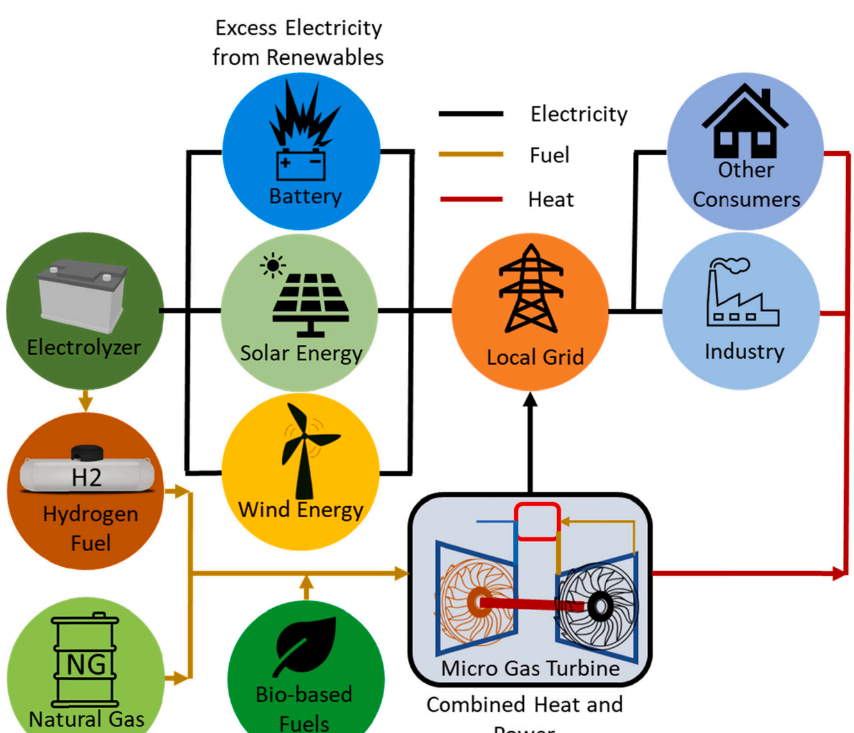

Fig. 1. MGT in hybrid integrated distributed energy network.

Overview of transient operations in MGT

Start-up sequencing

The start-up sequence of MGT consist of two most pivotal steps that are *cranking* and *ignition*. *Cranking* is performed by an alternator that works as a starter motor during start-up/shutdown, and acts as a generator during self-sustaining operation [6]. The self-sustaining condition is the equilibrium position at which the stimulating torque of the turbine and the opposing torque of the compressor and sliding bearing are both equal, and the motor and generator both generate zero output power [7]. Subsequently, the ignition is deployed after shaft speed reaches ~10 – 20% of rated speed, thereafter a main fuel schedule is activated to accelerate the MGT to the rated speed. Once the self-sustaining state has been achieved at ~65% of the rated speed, the starter cut-off is deployed. Additionally, fuel flow rate is one of the most crucial parameters to ensure a stable operation. Therefore, after reaching the self-sustaining stage, a sufficient amount of fuel must be provided to match the load; otherwise, rotational speed will be adjusted, potentially exceeding the speed restriction. Hence, forecasting fuel consumption range becomes important. Guan et al., [8] have developed a dynamic model to evaluate the self-sustaining performance during start-up of a self-designed 30 kW MGT. Self-sustaining transition boundary and associated self-sustained point were determined besides identification of the fuel consumption range. It was revealed that self-sustaining operation was closely tied to the shaft speed irrespective of the maximum level of fuel flow adjustment. The start-up operating regime of an MGT consisting of different phases, has been illustrated in Fig. 2.

Shutdown sequencing

The shutdown process in the MGT is normally attributed as the ramp down of the load to reduce the speed of the engine thereby disconnecting the MGT from the grid. During shutdown, load is initially reduced to roughly 20% of the nominal load, then it is ramped down to zero. Eventually, fuel is switched off after ~1.5 min of idle operation to cool down all the exhaust passages. The rotor then decelerates, relying solely on its residual rotational energy, and the thermal energy stored in the hot metal matrix [10]. The fuel valve tends to open during idle performance, while producing no power. This happens due to a decrease in natural gas delivery pressure, which is managed by the gas compressor. In general, rotor takes ~3.5 min to bring a complete stop from full load. The shutdown sequence of the MGT is shown in Fig. 3. It can be observed from the figure that shaft speed and turbine outlet temperature (TOT) are showing delayed responses to the shutdown command given by the

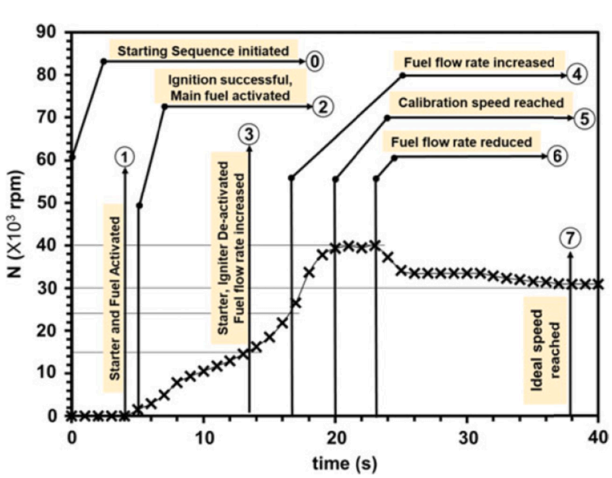

Fig. 2. Start-up sequence of an MGT, [9].

operator. Due to a sharp variation in the TOT, shutdown phenomena of the MGT are prone to fatigue failure of the hot gas path components such as combustor and recuperator. Hence, it is an imperative need to study the shutdown process both numerically and experimentally.

Load fluctuations due to RES integration

The transition from conventional energy systems to more sustainable ones requires utilization of RES. In hybrid integrated or fully RES-driven systems, the fluctuating nature of RES might require frequent load ramping during intermittency. Frequent load ramps might result in serious fatigue and creep failures. Hence, dynamic performance study of MGT accommodating the sharp accelerations and decelerations must be conducted.

Load changes have been accounted for by a few studies. For instance, Bracco et al., [11] have simulated the mid-season load variation in summer. In this regard, a dynamic simulation model of an MGT in a cogeneration plant was established to evaluate the part-load and transient performance of the cogeneration plant in a smart grid. The exhaust gas temperature and shaft speed are proved as a function of load. The load following dynamic phenomena of MGT is also affected by variable and constant shaft speed operating modes. That is why, Duan et al., [12] compared the nonlinear performance of the simple and recuperated MGT cycle at constant and variable speed mode. The study concluded that the recuperated MGT at variable speed mode was the optimally efficient cycle mode. However, the engine can face surging and increased turbine inlet temperatures (TIT) at low speeds during low loads. In another study Duan et al., [13] simulated the load change phenomenon for variable power steps. It was found that fixed step change interval over different equilibrium positions showed less overshoot, minimal oscillation, and quicker convergence during decreased loads. Whereas at increased load, these characteristics are considerably higher. Their study showed that dynamic characteristics at lower and higher loads have obvious distinction. The part-load phenomenon depicts different dynamics in grid connected and standalone mode. These operating modes can significantly alter the dynamics of the engine. The MGT connected to grid must work on a constant shaft speed to synchronize with the rated frequency of the grid (50 or 60 Hz) [14]. However, this constant shaft speed operation is not applicable for all the commercially available MGT due to presence of integrated power electronics that normally performs power conditioning to provide 50/60 Hz. On the other hand, in a standalone mode, there is a flexibility to change the shaft speed. The two operating modes are well described in the Fig. 4 [15].

In a grid connected case during part-load conditions, the shaft speed is increased and manifests an overshoot [15]. Similarly, during the standalone mode, the part-load operation smoothly follows the shaft speed; hence, reducing the pressure ratio of compressor and firing temperature of combustor. Subsequently, the shaft speed is recovered that reveals that surging in the compressor can occur. Fig. 4(a) represents a constant shaft speed scenario in which each change in fuel consumption (dotted pink line) and generator load coefficient, K, (solid coloured line) leads to a power un-balance. The 'K' can be estimated using Eq. (1). Similarly, Fig. 4(b) illustrates a variable speed scenario that is more favourable at part load operation. The reason lies in the fact that at the same power output the fuel flow rate is reduced that translates into increased thermal efficiency [15]:

$$\frac{P_{el}}{P_r} = K\left(\frac{\omega}{\omega_r}\right)^3 \tag{1}$$

Where the 'r' denotes the rated values for electric power (P) and shaft speed (ω) of MGT. Owing to the above-mentioned statements, higher levels of dynamics are raised due to over speeding resulting from higher values of fuel flow rates at point A1 and A2 as mentioned in Fig. 4(a). Therefore, study of transient phenomena of MGT at grid connected and

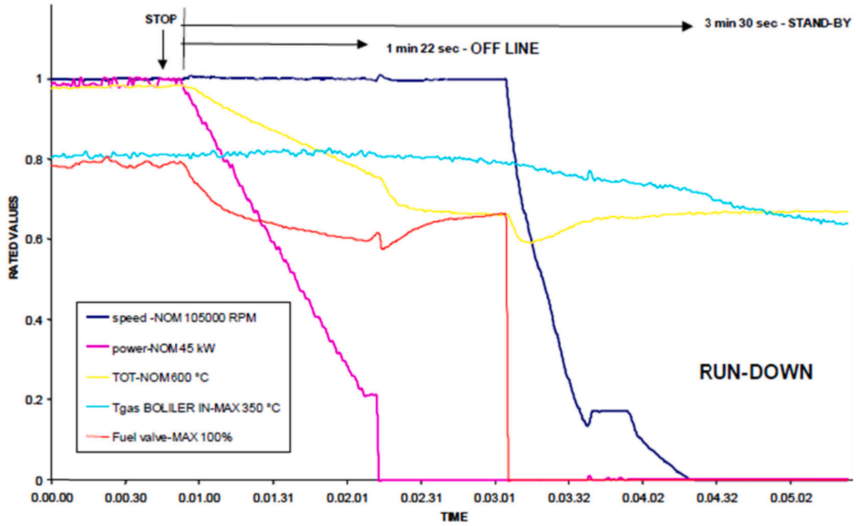

Fig. 3. Shutdown sequencing of the Bowman TG45 MGT, [10].

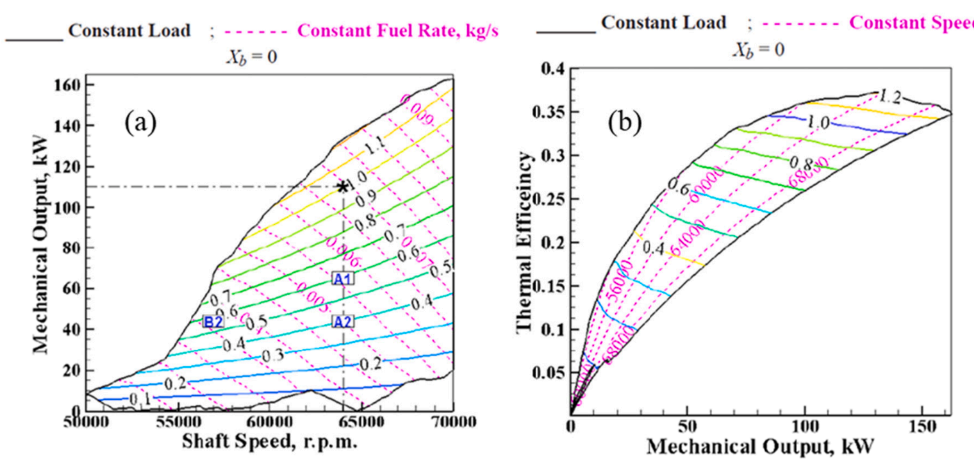

Fig. 4. The operating envelope of constant (a), and variable speed mode (b), [15].

standalone modes becomes imperative. However, the current literature has the scarcity of dynamic studies in such operating modes.

Dynamic performance studies

Analytical and experimental research on the dynamic behavior of gas turbines dates to the early 1950s, when the twin spool engine was first introduced. Nevertheless, the dynamic modeling of gas turbines using digital computers began in 1971, when Fawke and Saravanamuttoo developed a dynamic mathematical model of gas turbines [16]. Sellers and Daniele [17] from NASA developed a zero-dimensional transient simulation code named DYNGEN for the performance study of aircraft gas turbines. However, the dynamic performance simulations of smaller engines with radial type turbomachinery such as MGTs started in 1993 with the development of a transient model for solar powered regenerative MGT. This simulation model was developed with the help of mass, momentum and energy conservation equations and was able to predict the low frequency transients introduced by control system of the engine [18]. However, the dynamic simulation model of natural gas fueled recuperated MGT was firstly initiated in 2000 by Kim et al., [19]. This model was based on unsteady one-dimensional conservation equations implemented on constituent components assumed as finite control volumes. Although this model considered the thermal inertia of the recuperator, the heat soakage and volume dynamics were not considered. These limitations had been compensated in another code named TRANSEO that was also developed in the same year. The TRANSEO code was developed by Traverso for dynamic and transient performance study of energy systems [10]. It was a MATLAB-based modular and flexible simulation tool capable of simulating multiple models for all the components existing in its Simulink library. This software has considered both constant mass flow and lumped volume approach to capture the volume dynamics, while heat transfer from the fluid to the metal matrix and the environment have been considered as well. The code is capable of modeling various power cycles such as micro humid air turbine, externally fired micro gas turbine (EFmGT) and solar micro gas turbine [20]. The cogeneration energy systems incorporating the heat recovery boiler increase the overall efficiency of distributed energy systems. Therefore, Gambrotta et al., [21] developed a physics-based dynamic model for an MGT associated with a cogeneration energy system. The model was reported to be fast in numerical calculations; however, a proper experimental validation was missing. Apart from the in-house built codes, variety of commercial codes have been adopted in the literature to simulate transient operation of micro gas turbines. For instance, Chiang et al., [22] have employed GasTurb software to simulate the steady state and transient behaviors of a micro turbojet engine. The simulation results showed good agreement with experimental test campaigns data.

In addition to the pioneer dynamic modeling studies, some contemporary studies have also been published. Most recently, Gaitanis et al., [23] developed an experimentally validated transient performance assessment tool for a 100 kW MGT using Python programming language with an accuracy margin of 1.5% from the real data. The model was reported to be computationally efficient and less complex because of modular nature. Apart from considering natural gas as a fuel, recently there has been a progress in developing dynamic models for alternative fuel-based MGT. Banihabib and Assadi, [24] developed a model for 100 kW MGT using blends of hydrogen (80 vol%) and methane (20 vol%). The model was developed in MATLAB/Simscape commercial tool, and validation was conducted with the experimental data. The accuracy of the model was reported to be <8% compared to the real-time data. Similarly in another study conducted by Raggio et al., [25], the TRANSEO code was employed to investigate the effect of variation in fuel composition on the transient performance of a 100 kW MGT. The effect of different fuel blends (i.e., NH_3–NG, and H_2–NG) of diverse compositions on surge margin, TIT and TOT was studied. The H_2–NG blending case showed temperature rise with every 10% (vol.) increase of H_2. While in NH_3–NG blended fuel scenario, the surge margin exceeded beyond allowable limit at low power settings. However, at higher power settings, the surge margin (SM) was observed to be in the allowable range. He et al., [26] utilized a reinforcement learning identification approach to simulate the start-up and shutdown regimes of a 30 kW MGT. The critical transient parameters such as recuperator's thermal capacity and shaft moment of inertia were identified using reinforcement learning. Similarly, another study by Bozza and Tuccillo [15], established a transient model of a cogeneration system consisting of a partially recuperated MGT. The transient response of critical components such as combustor and heat exchanger were investigated during constant and variable shaft speed. Moreover, it was revealed that part to full load transient response based on predefined fuel schedule showed a sharp irregularity in the power unbalance that could lead to surging and choking of the compressor. Additionally, increasing controller constant lead to improved and smoother transient response. Henke et al., [27] developed a new dynamic modeling code in FORTRAN environment. This simulation tool was based on simplified physical modeling approach for recuperated MGTs. The tool is reported to be fast speed to capture the slow transient manoeuvres based on multimillion time steps. The heat transfer from gas to casing has a significant effect on the dynamic operation; that is why lower casing heat capacities were included.

After an extensive literature review it was inferred that, the literature encompasses dynamic performance studies of MGT ranging from 30 to 150 kW of power ratings while a single study considers radial turbomachinery-based 1,900 kW small gas turbine too. It was also revealed that, most of the dynamic performance studies are based on physics-based numerical simulations; however, there was a scarcity in the experimental dynamic studies of MGT. Moreover, the widely simulated dynamic regimes were start-up and load change while the shutdown regime remained shallow. Additionally, heat transfer transient effects have been accounted for sparingly. The dynamic performance studies based on hydrogen and NG blends were found to be infant. The detailed comparison of dynamic performance studies is demonstrated in Table 1.

Table 1
Dynamic performance studies for micro gas turbines in the literature.

Ref.	Engine type	Capacity	Transient operation	Methodology	Study type
[23]	Recuperated MGT	100 kW	Load change	Physics-based model using Python	Numerical
[24]	Recuperated MGT	100 kW	Load change	Physics-based model using Simulink/Simscape	Experiment and numerical
[28]	Recuperated MGT	100 kW	Load change	MATLAB/Simulink	Numerical
[8]	Simple MGT	30 kW	Self-sustaining start-up	Physical model	Experiment and numerical
[26]	Simple MGT	30 kW	Start-up and shutdown	Reinforcement learning-based identification approach	Numerical
[29]	Solar MGT	500 kW	Start-up and shutdown	Thermodynamic model using MATLAB/Simulink	Numerical
[30]	Simple MGT	30 kW	Transients involved with Electro-mechanical and Thermo-mechanical sub systems	Data-driven; particle swarm optimization assisted radial basis function	Numerical
[11]	Recuperated MGT integrated with HRB in cogeneration plant	65 kW	Mid-season load variation; summer peak load	Physical model with electrical analogy of capacitance and inductance for mass flow and kinetic energy accumulation	Numerical
[12]	Simple cycle and recuperated MGT	30 kW	Load change	Nonlinear analytical model	Numerical
[27]	Recuperated MGT	100 kW	Start-up, load change and shutdown	Physical model in FORTRAN environment	Numerical
[31]	Recuperated MGT in hybrid energy grid consisting of solar, PV and hydrogen	100 kW	Load change, ambient conditions, and fuel composition variations	Physical model with one dimensional ODEs	Experiment and numerical
[32]	Recuperated ultra-MGT	500 W	Start-up, self-sustaining and booster operation	Gasturb11 simulation software, fixed speed mode	Experiment and numerical
[33]	Small radial GT OP16	1900 kW	Load shedding	GSP software, thermal effects, heat soakage and volume dynamics	Numerical
[34]	Recuperated MGT	30 kW	Load following	Physical model	Numerical
[35]	Micro turbo jet	140–180 N	Heat transfer during shutdown (cooling process of engine)	3D CFD model using ANSYS; Numerical Conjugate model and heat transfer model	Experiment and numerical
[13]	Recuperated MGT	30 kW	load change	Nonlinear state space method using MATLAB/Simulink	Numerical
[36]	EFmGT coupled with ORC	70 kW	start-up, load change and shutdown	Conservation of mass, energy equations; thermodynamic equations	Numerical
[37]	Recuperated mHAT	100 kW	Load increased ramp and decreased ramp	TRANSEO code (physical model)	Numerical
[38]	Split shaft MGT generator	150 kW	Load following	MATLAB/Simulink	Numerical
[39]	Simple MGT	75 kW	Load change	Aspen-HYSYS, state space method (physical model)	Numerical
[10]	EFmGT	80 kW	Load change	TRANSEO code (physical Model)	Experiment and numerical
[40]	Recuperated MGT	100 kW	Start-up, shutdown, load following	Physical model (ICMF and lumped volume approach)	Numerical
[15]	MGT- cogeneration partially recuperated	110 kW	Load following	Physical model	Numerical
[19]	Recuperated MGT	100 kW	Periodic load following	Physical model	Numerical

Component-based dynamic modeling methods

Understanding the difference between transient and dynamic phenomenon is indispensable before starting the dynamic performance study of MGT. The transient performance is referred to as low frequency variations such as power excursions [41]. On the contrary, dynamic performance provides information about surging, rotating stall, and engine starting conditions. Normally in gas turbines systems, a frequency variation up to 5 Hz is termed as 'transient', whereas variations ranging between 30 and 50 Hz are considered as 'dynamic' frequency changes. This distinction might be beneficial for developing transient and dynamic models for MGT engines [42].

The dynamic performance studies pertinent to MGT are largely based on physics-based simulation models. The overall physics-based simulation models are developed with help of component-based thermodynamic modeling of constituent components. A typical MGT available in the market consists of following major components: compressor, turbine, combustor, recuperator, high speed permanent magnet synchronous generator (PMSG), electrical power invertor, and electronic control system. When it comes to dynamic physical modeling, only major components i.e., compressor, combustor, turbine, and recuperator have been considered by majority of the studies. However, a few studies have considered the rest of the components as well in their dynamic models. The schematic of MGT is shown in Fig. 5.

These models are approximated with the help of unsteady form of one-dimensional conservation of mass, momentum and energy equations implemented on each constituent component of MGT. To apply conservation equations, each component is assumed as a finite control volume. Some studies have incorporated all the three conservation equations, while a few have neglected the momentum equation and associated pressure wave propagation effects. The momentum balance equation is normally opted when there is a need to investigate surging due to pressure fluctuation in the compressor. The below mentioned equations represent the integral form of the conservation equations that are further converted to ordinary differential equations (ODEs) [43].

$$\int\left[\frac{\partial\rho}{\partial x}+\nabla.(\rho \mathrm{u})\right]dV=0 \tag{2}$$

$$\int\left[\frac{\partial(\rho u)}{\partial t}+\nabla.(\rho uu)\right]dV=-\int_S pndS+F \tag{3}$$

$$\int\left[\frac{\partial(\rho\hat{e})}{\partial t}+\nabla.(\rho\hat{e}\mathrm{u})\right]dV=\dot{Q}-\dot{W}_s-\dot{W}_p \tag{4}$$

$$\hat{e}=e+\frac{1}{2}(\mathrm{u.u}) \tag{5}$$

The unsteady form of MGT constituent components is described by the integration of above-mentioned conservations equations into ODEs as follows [43].

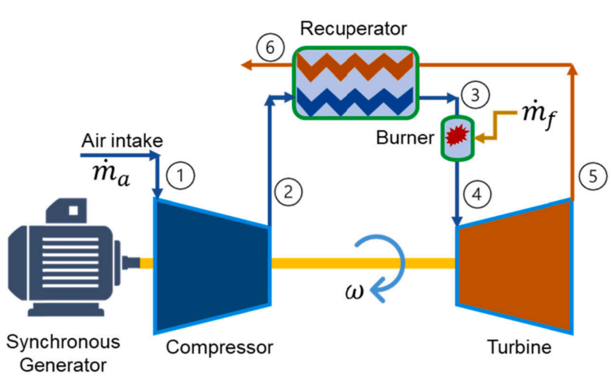

Fig. 5. Schematic of a recuperated MGT.

$$V\frac{d\rho_{i+1}}{dt}=-\dot{m}_{i+1}+\dot{m}_i \tag{6}$$

$$V\frac{d(\rho u)_{i+1}}{dt}=-\left(\dot{m}_{i+1}u_{i+1}-\dot{m}_iu_i+p_{i+1}A_{i+1}-p_iA_i\right)+F \tag{7}$$

$$V\frac{d(\rho H-p)_{i+1}}{dt}=-\left(\dot{m}_{i+1}H_{i+1}-\dot{m}_iH_i\right)+\dot{Q}-\dot{W}_s \tag{8}$$

The above-mentioned ODEs can be solved by using the given boundary conditions. Moreover, the above equations are implemented on every component with appropriate input values of $\dot{Q}$, $\dot{W}_s$, and F, for a specified time step. The $\dot{W}_s$, and F are obtained from performance map or off-design calculations. The outlet conditions of a control volume are obtained once the inlet conditions (pressure and temperature) are given. Subsequently, the following equations are employed to determine the force and shaft power [43].

$$F=\left(\dot{m}^*_{i+1}u^*_{i+1}-\dot{m}_iu_i+p^*_{i+1}A_{i+1}-p_iA_i\right) \tag{9}$$

$$\dot{W}_s=\dot{m}_i\left(H_i-H^*_{i+1}\right),\ \text{where}\ \dot{Q}=0 \tag{10}$$

The asterisk symbol represents the outlet conditions of the control volume at given inlet conditions for a specified time step. The further components methodologies are discussed in the following sections.

Inlet and exhaust ducts

During the physical model development, some assumptions are established to ensure simplifications in a mathematical model. To avoid complications, the inlet air temperature is normally assumed to be equal to the ambient temperature. However, there exists some discrepancy in them. Heat generated by the gas turbine and auxiliary systems in the machine enclosure causes an incessant increase in the temperature of the effective air entering the compressor stage. Therefore, to anticipate the MGT's response to temperature changes, the following correction factor is assumed [31].

$$T_i=T_a+\delta T_i \tag{11}$$

In the above equation, the δT_i is termed as the correction factor that is tuned by doing experiments. Apart from this, the total pressure loss in the inlet and outlet are normally corrected by the following equation [43].

$$\frac{\left(\frac{\Delta P}{P_{in}}\right)}{\left(\frac{\Delta P}{P_{in}}\right)_d}=\frac{\left(\dot{m}\frac{\sqrt{T}}{P}\right)^2_{in}}{\left(\dot{m}\frac{\sqrt{T}}{P}\right)^2_{in,d}}\times\frac{R}{R_d} \tag{12}$$

However, $\dot{Q}$, and $\dot{W}_s$, in Equation (8), are assumed to be zero during inlet and outlet duct modeling.

Turbomachinery

The turbomachinery components of MGT such as centrifugal compressor and radial turbine have a quick transient response in case of any external perturbation (i.e., start-up, shutdown, and load change). That is why, they have lower time constant as compared to the recuperator, combustor, and heat exchanger. In this regard, turbomachinery components are modeled based on quasi-steady state assumptions to avoid complications in the computational efforts of the simulation. This semi-steady assumption describes the turbomachinery components as steady state devices; hence, same methodology can be adopted for both steady and transient operation simulations. As shown in the equations below, basic thermodynamic equations of efficiency and work are utilized for design point calculations [34]:

$$\eta_{comp} = \frac{h_{out,s} - h_{in}}{h_{out} - h_{in}} \tag{13}$$

$$\eta_{turb} = \frac{h_{in} - h_{out}}{h_{in} - h_{out,s}} \tag{14}$$

$$\dot{W}_{comp} = \dot{m}(h_{out} - h_{in}) \tag{15}$$

$$\dot{W}_{turb} = \dot{m}(h_{in} - h_{out}) \tag{16}$$

The outlet temperature of compressor and turbine can be determined from the following equations once the inlet temperature and pressure ratios are known [44].

$$\Delta T_{comp} = \frac{T_{in,comp}}{\eta_{comp}}\left[\left(\frac{p_{out,comp}}{p_{in,comp}}\right)^{\frac{k-1}{k}} - 1\right] \tag{17}$$

$$\Delta T_{turb} = \eta_{turb}.T_{in,turb}\left[1 - \left(\frac{p_{out,turb}}{p_{in,turb}}\right)^{\frac{k-1}{k}}\right] \tag{18}$$

Although, majority of the studies have assumed quasi-steady equations for compressor and turbine, Rossi et al. [44] have utilized a time decay term, initially introduced by Traverso, to simulate the dynamic characteristics of the compressor triggered by the load dependent time constant (τ). The outlet temperature of the compressor during dynamic operation has been characterised by the following equation [44].

$$T_{out,comp}(t) = T_{in,comp} + \Delta T_{comp}\left(1 - e^{-\frac{t}{\tau}}\right) \tag{19}$$

The off-design performance of the MGT is simulated by employing turbomachinery performance maps provided by the manufacturer to capture the performance of the MGT over a wide range of operating conditions (i.e., variations in ambient conditions, load, and fuel composition). Most of the time due to unavailability of the performance maps by the manufacturer, automotive turbochargers' performance maps are adopted for simulations purposes. The performance maps depict pressure ratio and isentropic efficiency as a function of corrected mass flow and corrected shaft speed, as shown in Fig. 6.

Combustor

The combustor is the most pivotal component for conversion of fuel's chemical energy to thermal energy to drive the turbine. The modeling of combustor for MGT is carried out by assuming a constant volume single cylinder device. Since there is no work involved in the combustion process, only heat transfer is considered in the energy equation. The amount of heat exchange is calculated using the equation below [43]:

$$\dot{Q} = \eta_{comb}\dot{m}_f\left(LHV + \Delta H_{T_0 - T_f}\right) \tag{20}$$

The subscript '0' in the above-mentioned equations represents the reference value for defining the lower heating value (LHV) of the fuel. The mass conservation equation implemented on the combustor accounts for the fuel flow rate along with air mass flow rate in the following expression:

$$V\frac{d\rho_{i+1}}{dt} = -\dot{m}_{i+1} + \dot{m}_i + \dot{m}_f \tag{21}$$

Additionally, the pressure loss during the off-design conditions is corrected using the following equation [43]:

$$\frac{\left(\frac{\Delta P}{P_{in}}\right)}{\left(\frac{\Delta P}{P_{in}}\right)_d} = \frac{\left(\dot{m}\frac{\sqrt{T}}{P}\right)^2_{in}}{\left(\dot{m}\frac{\sqrt{T}}{P}\right)^2_{in,d}} \times \frac{R}{R_d} \tag{22}$$

Recuperator

Heat exchange between hot gas and cold air in a recuperator is a sluggish process resulting in a slow change rate of cold end temperature. As a result, the dynamic response of a regeneration cycle is slower than that of a simple cycle. The reason for this is essentially the thermal inertia of recuperator in recuperative cycles [13]. A small heat exchanger, which can be either a static recuperator or a rotating regenerator is typically used in recuperated MGTs. Most of commercially available MGTs are outfitted with a static recuperator. While thermodynamic specifications for the recuperator were provided at the preliminary design stage, the manufacturer has yet to properly determine geometric data. In this context, the geometry and performance data of a plate-fin and counter flow type compact heat exchanger commonly employed in miniature regenerative gas turbines is assumed for modeling purposes [19]. In addition to this, most early models of MGT divided the recuperator in small finite segments associated with lumped volumes for better simplification of recuperator's metal. Heat transfer phenomenon is addressed in the governing equations of the recuperator, as follows [19]:

$$V\frac{d}{dt}(\rho H - p)_{a,i+1} = -\left(\dot{m}_{i+1}H_{i+1} - \dot{m}_iH_i\right)_a + \alpha_aA_w\left(T_w - \overline{T}_a\right) \tag{23}$$

$$mc\frac{dT_w}{dt} = \alpha_aA_w\left(\overline{T}_a - T_w\right) + \alpha_gA_w\left(\overline{T}_g - T_w\right) \tag{24}$$

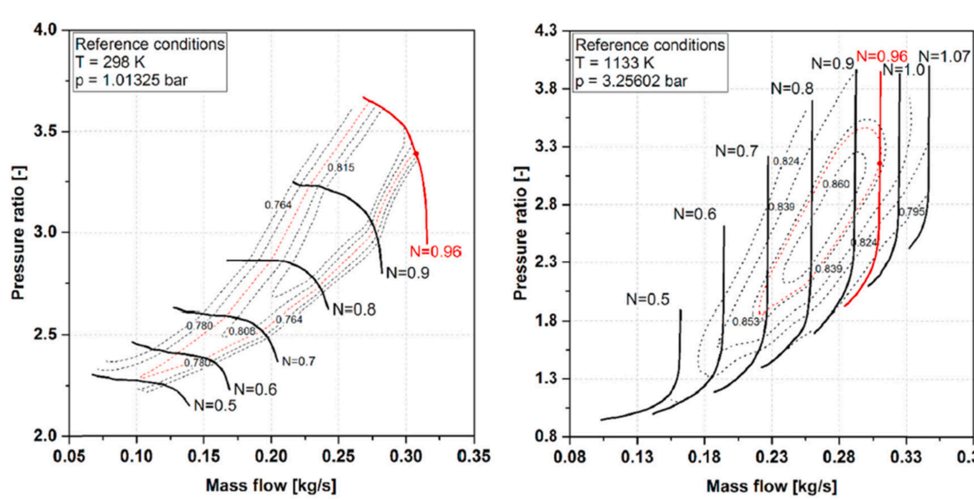

Fig. 6. Compressor (left) and turbine (right) performance maps of C30 MGT, [45].

$$V\frac{d}{dt}(\rho H - p)_{g,i+1} = -\left(\dot{m}_{i+1}H_{i+1} - \dot{m}_i H_i\right)_g + \alpha_g A_w\left(T_w - \overline{T}_g\right) \tag{25}$$

Whereas m and c are the mass and specific heat capacity respectively while $\overline{T}$, is the average temperature.

Multi-segment 1-D approach

Kim et al., [34] neglected the volume dynamics (fluid inertia) by assuming the quasi-steady approach. Moreover, they also utilized the finite segments approach (n_x) by distinguishing cold side form hot side with a recuperator wall in the middle, as shown in Fig. 7.

The governing equation of the fluid heat transfer is based on differential energy equation as follows [34],

$$mdh = dA\alpha\left(T_{HX} - T_{flow}\right) \tag{26}$$

$$\dot{m}_c\left(h_{c,l+1} - h_{c,l}\right) = \frac{A}{n_x}\alpha_c\left(T_{HX,l} - \frac{T_{c,l+1} + T_{c,l}}{2}\right) \tag{27}$$

$$\dot{m}_h\left(h_{h,l+1} - h_{h,l}\right) = \frac{A}{n_x}\alpha_h\left(\frac{T_{h,l+1} + T_{h,l}}{2} - T_{HX,l}\right) \tag{28}$$

$$\frac{A}{n_x}\alpha_c\left(T_{HX,l} - \frac{T_{c,l+1} + T_{c,l}}{2}\right) + \frac{A}{n_x}\alpha_h\left(\frac{T_{h,l+1} + T_{h,l}}{2} - T_{HX,l}\right) = \frac{(mc)_{HX}}{n_x}\frac{T^t_{HX,l} - T^{t-1}_{HX,l}}{\Delta t} \tag{29}$$

Kim et al., [34] has replaced the enthalpy terms with '$c_p\Delta T$' to reduce the complication caused by multidimension and nonlinear nature of the governing equations involved in calculations through Newton-Raphson solver. Although this approach has helped in linearization of the equations, it has the drawback of bringing inaccuracy in the energy equation due to presence of the $c_p\Delta T$ term. This can only be compensated by dividing the volume in several segments for a continuous variation of heat capacity along with flow direction, hence, reducing the relative error of inaccuracy. Since the specific heat is a temperature dependent parameter, it continuously changes with time. Therefore, an iterative calculation methodology is adopted for a good convergence in dynamic simulations. Additionally, the number of iterations can be reduced significantly by reducing the time step during the dynamic simulations.

Discrete volume thermal mass approach

Henke et al., [27] have introduced an approach by dividing the recuperator in discrete cells and thermal masses of tubular shapes. The discrete cells represent mass and heat flow of gas, while thermal masses (TMs) represent the metal heat transfer sheet, as shown in Fig. 8. The cells transfer the heat to the thermal masses and a heat flow process goes on. The thermal masses help in heat transfer via two modes i.e., heat flow through conduction to recuperator casing and insulation, as well as free convection to the ambient air. The equation of conduction is given below as [27]:

$$\dot{Q} = \frac{2\pi.L.\lambda_{tm,inner}.\lambda_{tm,outer}.\left(T_{tm,inner} - T_{tm,outer}\right)}{ln\left(\frac{r_{tm,outer}}{r_{tm,outer} - d_{tm,outer}/2}\right) + ln\left(\frac{r_{tm,inner} + d_{tm,inner}/2}{r_{tm,inner}}\right)} \tag{30}$$

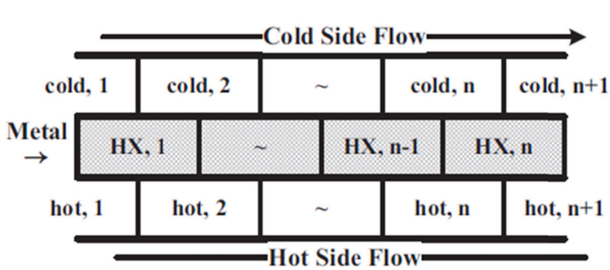

Fig. 7. Multi-segment heat exchanger, [34].

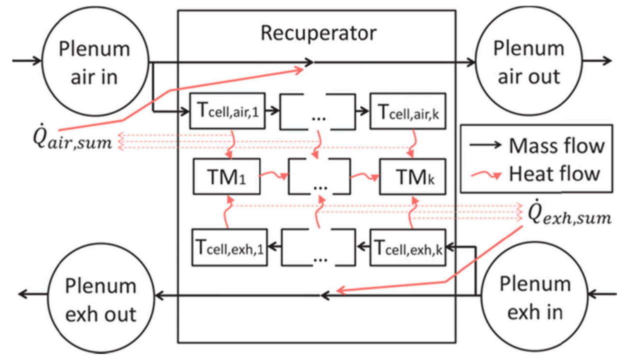

Fig. 8. The recuperator concept of heat transfer via thermal masses, [27].

where the subscripts '*inner*' and '*outer*' denote the inner and outer radius surfaces of the tubular thermal masses. The convection heat transfer equations are as follows [27]:

$$\dot{Q} = \frac{\alpha_{cond}.\alpha_{conv}}{\alpha_{cond} + \alpha_{conv}}.(T_{tm} - T_{amb}) \tag{31}$$

where,

$$\alpha_{cond} = \frac{L.2\pi.\lambda_{tm}}{ln\left(\frac{r_{tm}+d/2}{r_{tm}}\right)} \tag{32}$$

$$\alpha_{conv} = \frac{Nu.\lambda_{amb}.S}{L_{chara}} \tag{33}$$

In the above equation, S represents the outside surface area, and L_{chara} is the gas path length along the surface area. However, access to these kinds of data is barely provided by manufacturers. Therefore, these parameters are based on assumptions and approximations from the external dimensions.

Volume dynamics

The response delay of the MGT during external perturbations is characterized by many types of inertias such as fluid inertia. During the dynamic excursion, the incoming fluid mass flow of a certain constituent component is not equal to the outgoing mass flow. In fact, some of the fluid mass is accumulated in the gas path components leading to a mismatch of conservation of mass equation. This phenomenon is known as volume dynamics or gas dynamics. Alves and Barbosa [42] have defined the frequency range for this kind of dynamic phenomenon as 5–50 Hz. In general, two kinds of approaches have been established in the literature. Fawke and Saravanamuttoo have introduced the concept of iterative constant mass flow (ICMF) and inter-component (ICV) volume methodologies [16]. According to the ICMF method, the incoming fluid mass flow in any control volume is equal to the outgoing mass flow, as reported by Davison et al., [46]. This method has been assumed by variety of researchers in order to reduce the computational efforts of the iterative solver. The wide adaptability of this method is due to its larger time steps during iteration to converge the solution. On the contrary, in the ICV method, the flow is not conserved and pressure rise inside a constituent components' control volumes can typically occur during real transient operations [47]. Some researchers have considered quasi-steady assumptions of the constituent components during modeling.

To account for the fluid inertia effects during transient operation, smaller volumes are introduced between the two consecutive components. This is sometime named as lumped volume approach (LVA) [10]. The physical meanings of both ICV and LVA are quite similar. The topic of discussion is between the ICMF and ICV. The literature manifests that the ICMF and ICV are same in terms of computational efficiency. However, the ICV method has a priority due to establishing a smoother operating line trajectory on the turbomachinery performance maps during sharp transient excursions. In this regard, Kim et al., [48] developed a transient simulation model for an MGT auxiliary power unit that is typically used to start the helicopter engine. The effect of volume dynamics was investigated by attaching an intercomponent volume to the compressor exit. It was revealed that increase in the air volume of the volume plenum during step decrease in fuel flow resulted in surging of the compressor and led to instability of the engine. Hence, it was suggested to incorporate blow-off valves for a volume greater than 2 m^3 to avoid surging. The hypothetical volume plenum introduced downstream of the compressor can be regarded as the recuperator volume in case of micro-CHP systems. The volume dynamic concept has been comprehensively explained in a study by Hashmi et al., [49].

Thermal dynamics

Thermal dynamics or heat soakage effect is a phenomenon of heat accumulation inside the MGT and heat dispersion from the hot gas within the gas turbine to the surroundings through the component casing during dynamic operation. In a steady-state operation, heat transfer to the ambient is considered as constant. However, in transient operation, the component casing and related structure show delayed responses to heat up (or cool down) depending on their heat capacities. Although, these thermal effects are normally minor in heavy duty gas turbines, they can have a considerable impact on engine performance in MGT due to enhanced temperature differences in small distances owing to compact nature of turbomachinery [33]. The thermal dynamic phenomenon has a frequency range of 0–1 Hz, that must be taken into consideration for developing accurate dynamic models [42].

The shutdown operation is among those transient regimes that could reduce health of the engine components. The accumulated heat is distributed throughout the engine parts and dissipated into the atmosphere in the wake of an emergency or planned engine stop. It could potentially have a multifaceted impact on the bearings. Accumulated heat can lead to overheating and a significant temperature difference between the inner and outer races resulting in radial bearing clearance changes. The leftover oil in the bearing races can get coked at high temperatures [50]. The additional mass unbalance is caused by non-uniform buoyancy-governed natural cooling of the engine parts. Aside from that, natural cooling can produce non-uniform stiffness of the bearing support, bearing misalignment, and a reduction in radial clearances between rotating parts and the housing during engine hot start phase.

The thermal dynamics in MGT is normally accounted for by using conjugate heat transfer approach as suggested by Verstraete et al., [51]. Similarly, Tisarev et al., [35] have developed a 3-D, conjugate heat transfer model using ANSYS CFX, for a micro turbojet engine in order to investigate the heat transfer effects during rundown operation. It was concluded that radiation and forced convection significantly reduced temperature during the cooldown process. If the engine is restarted without a stipulated cooling duration the bearing rings can fail due to exceeding their tempering limit. Eventually, early failure can occur. The thermal dynamics during cooldown process of the engine requires conduction, radiation and convection equations, as follows [35]:

$$-\lambda_m\left(\frac{\partial T}{\partial x}\right)_m = h\left(T_m - T_f\right) + \sigma\left(T_m^4 - T_0^4\right) \tag{34}$$

Heat is normally, released in the ambient through radiation and convection; specifically forced convection during cooldown and natural convection during rotor stoppage. The natural convection is determined by *Nu* that is a function of Rayleigh number, given as follows [35].

$$Nu = \frac{\alpha D}{\lambda_f} = f(Ra) = f(Gr.Pr) \tag{35}$$

where,

$$Gr = \frac{gD^3}{\nu^2}\beta\left(T_m - T_f\right) \text{ and } Pr = \frac{c_p\mu}{k_f} \tag{36}$$

Shaft dynamics

Mechanical inertia of the shaft is responsible for delayed dynamic response of the MGT. Although, the time constant of the rotor shaft is lower as compared to the recuperator and combustor, shaft dynamics has a substantial impact on the overall safety of the MGT. In general, during load variation, the generator torque and rotor torque undergo a mismatch that leads to fluctuation in rotating speed of the shaft. Therefore, the following shaft dynamics equation is used to evaluate the mechanical inertia of the shaft [34].

$$\omega^{t+1} = \omega^t + \omega^t\frac{\Delta t}{I}\left(\dot{W}_s - \dot{W}_{ld}\right) \tag{37}$$

where,

$$\dot{W}_s = \dot{W}_{turb}\eta_{mech} - \dot{W}_{comp} \tag{38}$$

Control strategies

Effective control strategies are essential for a smooth and safe operation of MGTs, more specifically during transient operations. Typically, two types of control schemes are adopted for MGTs, i.e., prime control and protective control. These schemes are specific to the application for which an MGT is installed. For a grid connected engine, the purpose of the prime control is to maintain the frequency of the MGT in compliance with the required operating frequency of the grid by correcting the frequency changes instantaneously [52]. The protective control, however, ensures the safety of the engine during the event of torque fluctuations triggered by an external load. Therefore, the protective control decelerates the MGT during over speeding and over temperature to ensure overall safety of the engine.

Variety of control strategies exist in the literature in the domain of the heavy-duty industrial gas turbines (IGT). Nowadays, improved versions of the Rowen's transfer function model are widely used in the control system design of both IGT and MGT [53]. Although this model was developed originally for IGT, it is also applicable for MGT due to having a similar configuration (i.e., single shaft). The proposed simplified model provides control for speed, temperature, acceleration, and maximum fuel limit. In this regard, the model incorporated simple proportional (droop) and proportional-integral (isochronous) control schemes [54]. However, for MGT, the default control scheme is based on proportional-integral-derivative (PID) controller that adjusts the shaft speed according to the set point given by the operator. Additionally, to meet the designated material temperature limit of the turbine, the TOT is adjusted by manipulating the fuel flow rate. This default control

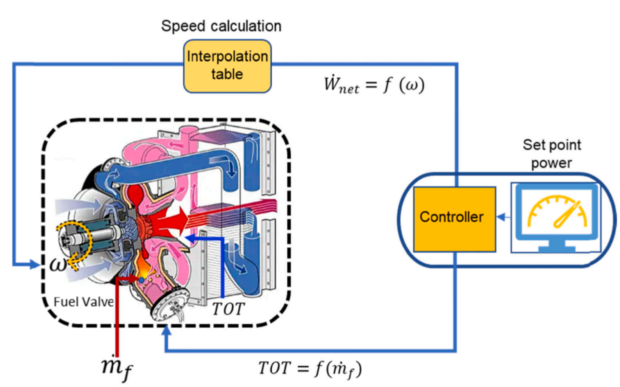

Fig. 9. Default control scheme in MGT.

scheme has been illustrated in Fig. 9. Nevertheless, in the past two decades, some new control models pertinent to MGT, have also been established. For instance, proportional-integral (PI), proportional-derivative (PD), model predictive control, genetic algorithm (GA) optimized PID controllers, fuzzy PID controller, and adaptive PID controllers. Further details are given in the subsequent sections.

Classical controllers

The PID, cascaded PI and simple PI and PD type controllers developed for MGT applications have been attributed as classical controllers in the present review. The PID controller typically modulates the error signal to meet the demanded output in the event of disturbances. The proportional terms reduce the error in the demand and the actual value, however, cannot reduce it to zero. The integral control adds the oscillations but synchronizes the demanded and actual signals. The derivative part of the PID decrease the oscillations and ensures stability, while fully modulating the error signal. The PID controller is very simple and is considered linear in nature; hence, it might compromise the stability in nonlinear dynamic systems such as MGT [55]. Moreover, noise and step changes in the demand can make the derivative part sensitive by triggering impulse in the control signal. Therefore, tuning the controller gains is needed to avoid the impulse in the signal.

Kim et al., [19] utilized Rowen's [53,54] isochronous governor model and transformed it into a PID controller with optimized control gains suitable for MGT transient conditions. It was observed that the uncontrolled recuperated MGT showed increased settling time with considerable overshoots and undershoots in shaft speed and TIT, respectively. Moreover, in the absence of PID controller, un-recuperated and recuperated cases showed a significant time lag due to thermal inertia of the recuperator. Similarly in another study, Kim et al., [34] used a PD controller for a recuperated MGT working on a variable speed mode in part-load operations (see Fig. 10). The PD controller aided in keeping the TOT constant during sudden load variations. However, a small discrepancy in real and simulation results was observed in the manipulated variables i.e., fuel flow and shaft speed due to control sensitivities. The deviations could be improved by using advanced control methods.

In addition to the general control schemes for recuperated MGT, some other control strategies for advanced cycles exist in the literature. De Paepe et al., [56] have developed a control strategy for saturation tower of a 100 kW micro humid air turbine (mHAT). The aim of the paper was to assess the accurate relative humidity of the compressed air leaving the saturation tower. Therefore, to optimize the cycle performance a control matrix was suggested to control TOT and power output for a fully air saturated mHAT. To ensure the overall conventional control of the MGT, an original electronic control unit (ECU) along with manual experimental control of water injection circuit was used. Similarly, Yang et al., [57] implemented two types of control schemes in a power regulated dynamic model for a 10 kW solar MGT. During the event of power regulation, PI and cascaded PI controller were developed to maintain the constant shaft speed and TOT, respectively. Hence, it was inferred that the constant TOT operation led to storage of 32% more energy than constant speed operation. The control system ensured an anti-surge and anti-stall operation of turbomachinery components. However, the adoption of control methods such as multi-variable constrained control, as well as experimental realization of the control system could have led to more improved results.

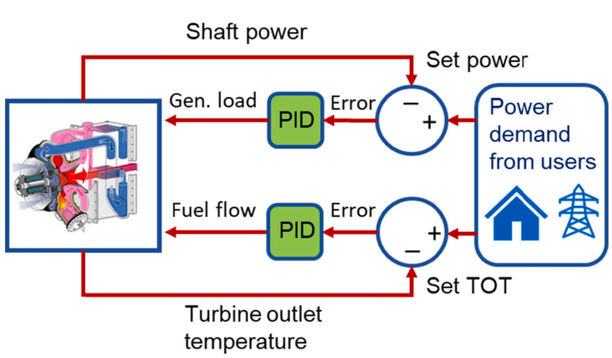

Fig. 10. PID control scheme for an MGT.

An in-depth survey of the literature reveals that several studies have incorporated PI controllers along with physics-based simulation models for MGT. However, PID controllers have also been used in some studies. Additionally, a few authors have considered PD and proportional feedback control schemes. Two of the studies have simultaneously used PI and PID for their dynamic models. The details of the classical controllers along with control parameters are listed in Table 2.

Advanced controllers

The present review has classified the model predictive control (MPC), adaptive controllers, artificial intelligence-based controllers, and some other controllers as the advanced controllers. The details are mentioned in the following subsections.

Model predictive controllers

Model predictive control is an effective control method for multivariable systems that meets a set of constraints. In MPC, the discrepancy between the anticipated output and the intended reference is reduced online across a future horizon, while the manipulated inputs, system outputs, and states are all constrained. It is a viable control strategy when a system is highly nonlinear or encompasses highly coupled control variables such as in combined cooling, heating, and power (CCHP) units and hybrid systems like MGT integrated with solid oxide fuel cells (SOFC). Therefore, it enables the optimization of the control trajectory based on various scenarios [60]. MPC employs quadratic cost functions as a typical technique to define the cost function minimizing the error between future outputs and desired values [61]. The output error e_y (between controlled variables and targets), the manipulated variables (MV), and the change rate of manipulated variables are the three terms in the cost function [62].

$$J = W_j^{e_y} S_{e_y}(z)^2 + W_j^{MV} S_{MV}(z)^2 + W_j^{\Delta MV} S_{\Delta MV}(z)^2 \tag{39}$$

Each term in the above equation is treated differently by the weights

Table 2
List of classical controllers in dynamic performance studies.

Author	Year	Control technique	Control parameters
Banihabib and Assadi [24]	2022	PI	TOT and power
Zhang [58]	2021	PID	Temperature and speed
Cameretti et al., [59]	2018	PI	Speed and air/fuel ratio
Bracco and Delfino [11]	2017	PI	Power and temperature
Henke et al., [27]	2017	PI and PID	Shaft speed and TOT
Kim et al., [34]	2016	PD	Shaft speed and TOT
Srikanth et al., [14]	2016	PI	Frequency and voltage
Duan et al., [13]	2015	PI	Speed
Barsali et al., [36]	2015	PI	TIT and power
Carrero et al., [37]	2015	PI and PID	TOT and power
Shankar and Mukherjee [38]	2014	PI	Speed and voltage
Traverso et al., [10]	2005	PID	Shaft speed and TOT
Traverso [40]	2005	PID	Shaft speed and TOT
Bozza and Tuccillo [15]	2005	Feedback proportional	–
Kim et al., [19]	2000	PID	Shaft speed and TOT

W_j. Although, the weights for MV and MV change rate are kept constant, the weights for output error are adjusted based on the predicted surge margin. Zaccaria et al., [62] employed an observer-based adaptive MPC associated with a model-based diagnostic tool to regulate TIT and surge margin at a safe limit ensuring the overall reliability and safety of MGT. The diagram is shown in Fig. 11. Although the model can predict sudden performance degradations of constituent components of MGT along with sudden spikes in SOFC pressure losses, the model can be improved by incorporating real-time performance degradation data of multiple components, simultaneously.

Zhu et al., [63] have developed two kinds of MPCs i.e., a coordinated MPC and a double MPC, for an effective control of a CCHP unit. Since a CCHP has high coupling, inertia and multiple variables, the implementation of conventional single input and single output-based PI controllers is not sufficient. Therefore, an MPC was adopted. The prediction model employed subspace identification (SID) to identify a state-space model that is derived from system's input–output data. The study revealed that a double MPC was capable of controlling temperature of hot and cold water, while a coordinated MPC could effectively control the shaft speed. The results of output parameters were compared with use of a conventional PID controller. The MPC-based control strategies showed stable dynamic responses, as compared to when a PID is employed, as shown in Fig. 12. Similarly, Wu et al., [64] also utilized the same SID technique to predict the control performance merely based on the data and without developing any model. This data-driven predictive control (DDPC) approach saves the time in developing complex MPCs, and greatly reduces the model mismatch events that can degrade the controller performance. The DDPC were compared to decoupled PI controllers. It was revealed that the shaft power showed an irregular behavior triggered by the disturbance in the presence of PI controllers, while the DDPC showed a great stability in the dynamic response, as shown in Fig. 13.

Shixi et al., [65] investigated the effect of ambient conditions on the control performance using an MPC for a MGT-PV-battery hybrid energy system. The MPC was compared with conventional rule-based control (RBC) logic. It was concluded that the use of MPC for power management in hybrid systems helps in minimizing the system cost and saves the fuel by 5% and 2.5% during summer and winter, respectively.

Artificial intelligence-based controllers

Advanced controllers are needed to deal with highly nonlinear, time variant and larger delay timing attributes of MGTs. The advanced controllers are normally developed by tailoring the existing control schemes to specific applications by modifying the controller gain parameters. Nowadays, artificial intelligence (AI) techniques based on fuzzy logic, genetic algorithm (GA), particle swarm optimization (PSO), and cuckoo search algorithms are used to tune the classical controllers. For instance, fuzzy control has been frequently employed in systems with uncertain models and non-linearities because it can deal with changes in system parameters. Fuzzy logic can be used to dynamically modify the settings of a PID controller, improving its performance and providing a reference for a nonlinear system's controller design. Yang et al., [55] have implemented a fuzzy PID (FPID) controller to an MGT engine for the first time. The control gains of the FPID were tuned with a novel hybrid approach by combining a PSO algorithm and a cuckoo search algorithm for better optimization of the control parameters. It was concluded that the new method achieved more robust stability and safety by enabling rapid responses to fuel flow, negligible overshoots and decreased stabilization times during load changes or external conditions variations. Moreover, FPID proved to be more effective over conventional PI and PID controllers. The performance of the controller is illustrated in Fig. 14. Although, the proposed technique gives improved dynamic control performance of MGT, it takes considerable time for calculation. Therefore, there is a need for further speed improvement of the technique.

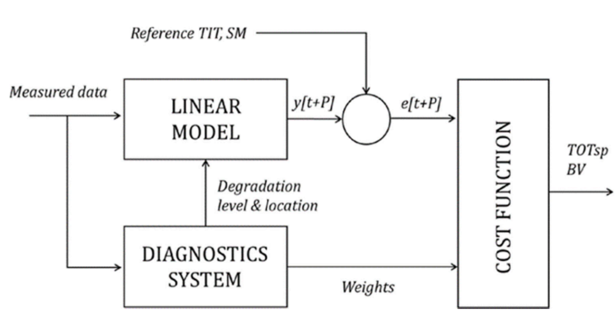

Fig. 11. The MPC associated with diagnostic tool, [62].

Similarly, Moustafa and Hassan [66] have compared the performance of classical and evolutionary computational technique-based controllers to figure out their suitability for grid-tied and islanded MGTs during load change conditions. It was revealed that PSO-fuzzy PD and adaptive accelerated coefficient PSO (AACPSO)-fuzzy PD showed optimum values for overshoot and settling time as compared to other controllers. The proposed control techniques are reported to be easy to implement without requiring detailed information about system parameters.

The controllers that utilize evolutionary algorithms for optimization of the existing classical controllers are known as optimized controllers. As already mentioned, the modified and modulated controller gains are needed for complex dynamics of MGTs. In this regard, a study by Alizadeh et al., [67] utilizes the genetic algorithm to tune the controllers' parameters of PI controller. The GA-based controller gain parameters offered an optimized controller performance of grid connected MGTs. Moreover, the speed control was achieved by a lead-lag transfer function-based model using MATLAB/Simulink tool. The model showed an improved controller performance.

Adaptive controllers

The adaptive controllers are typically suitable options where the systems operating characteristics change over time, or the uncertainties are unknown in the beginning. These online adjustable controllers can regulate their parameters in accordance with systems' varied operating conditions and expected uncertainties. Gain scheduling control is also a type of adaptive control that can continuously modify the gains of the controllers over the entire operating envelope of the MGT due to inherent nonlinear dynamics.

Deng and Zhang [68] employed an adaptive neural network (NN)-based fuzzy controller. In this technique, initially a PID controller was developed using Rowen's transfer function parameters and then it was tuned with fuzzy logic. The obtained FPID was then used to develop fuzzy neural network controller (FNNC) via a prediction model. The schematic of an adaptive FNNC is illustrated in Fig. 15. The fuzzy neural network (FNN) adaptive controller was compared with fuzzy logic controller and fuzzy PID controller. The FNN adaptive controller showed increased effectiveness and robustness for speed control.

Wang et al., [69] proposed a self-adaptive PID controller whose controller gains were tuned with back propagation (BP) neural network. The adaptive PID controller showed shortened governing time for exhaust temperature control during disturbance. The schematic of the adaptive PID controller is illustrated in Fig. 16. In another study, Wang et al., [70] utilized radial basis function (RBF) neural network (NN) for self-adapted tuning of classical PID controller to cope with the nonlinear dynamics of the MGT, effectively. Yet another study by Wu [71] used also the same technique. It was revealed that RBF PID had smaller overshoot as compared to other conventional controllers. Moreover, step response and anti-disturbance of RBF-tuned PID was smoother than that of simple PID controller, as shown in Fig. 17.

Other controllers

Several studies have employed the PI controllers for dynamic

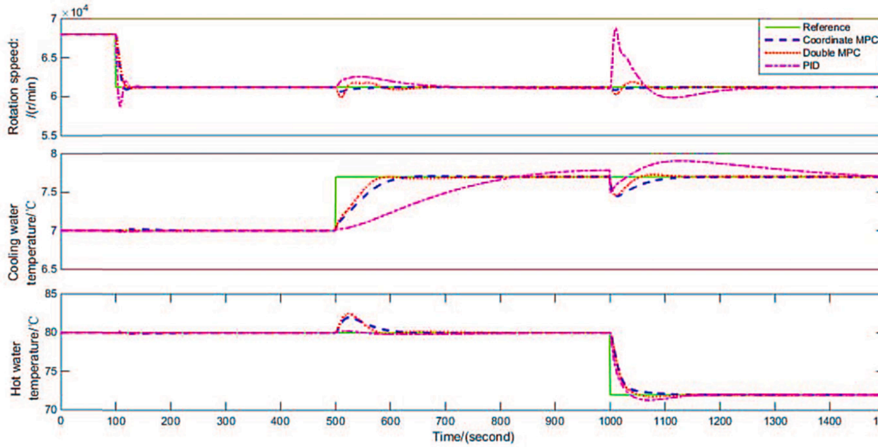

Fig. 12. Comparison of MPC and PID controllers for CCHP system, [63].

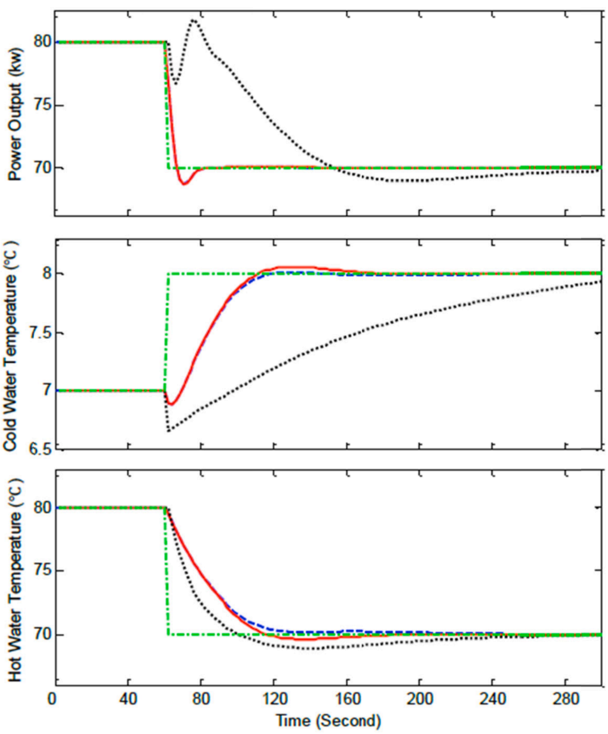

Fig. 13. Performance of CCHP system (red: DDPC, black: decoupled PI, dashed blue: MPC, and green: reference), [64]. (For interpretation of the references to colour in this figure legend, the reader is referred to the web version of this article.)

modeling of the MGT. However, the simple PI controllers consider the linearized modeling approach that creates oscillations in PI due to linearization errors; hence leads to internal disturbance. On the other hand, power production by MGT is termed as an external disturbance. The classical PI and PID controllers consider error elimination approach to curtail the effect of these disturbances. This disturbance reduction method is known as passive disturbance rejection. To obtain a higher controller performance with less oscillations, an active disturbance rejection control (ADRC) is normally utilized for many energy systems. In this regard, Lin et al., [72] adopted an ADRC for a simple MGT for the first time. The tracking differentiator, extended state observer (ESO), state error feedback rule, and disturbance compensation are all part of the ADRC. It performs the solution via the following formula [72]:

$$\dot{y}_n = \gamma^n \psi\left(y_1 - x, \frac{y_1}{\gamma}, \cdots, \frac{y_n}{\gamma^{n-1}}\right) \tag{40}$$

In the above equation, x denotes the input of the tracking differentiator, y represents the outputs, and γ is the variable factor coefficient. The above equation performs the solution that converges from y_1 to x. Nevertheless, ESO is the vital part of the ADRC that not only restructures the system's states, but also evaluates the total disturbance during dynamic operation. In the study by Lin et al., [72], three kinds of controllers i.e., nonlinear ADRC (NADRC), linear ADRC (LADRC) and PID were compared, as shown in Fig. 18. It was concluded that NADRC was the best control scheme due to incorporation of nonlinear error state feedback control law with nonlinear observer, as compared to passive disturbance rejection of PID control.

Wei et al., [73] proposed a double sinusoidal pulse width modulation (SPWM) control strategy for a MGT connected to a power converter interface in a grid connected mode. The effect of load change on both mechanical and electrical components was investigated using PCAD/EMTDC software tool. When a MGT system is used in a stand-alone microgrid mode, retaining load voltage and meeting power demand during load fluctuations is somehow critical. To keep the load-side voltage stable in a desirable range, an SPWM voltage management approach using a PI voltage regulator is used. The results reveal that the created model of MGT can swiftly control power output to satisfy load fluctuations' requirements, withstand sudden changes under normal conditions, and preserve specified voltage values. Although this model is capable of effective control, the recuperator dynamics is missing it does not seem suitable for start-up operation. Another technique that also considers the power electronic interface with mechanical components was proposed by Li et al., [74]. The proposed technique is known as causal graphing order approach that models the MGT and includes the controller. A graphical representation of all transferred physical parameters is used to model each component of MGT. However, the validation of the model was not presented in the aforementioned study. Table 3 lists a comparison of various advanced controllers in the literature.

Dynamics of innovative MGT cycles

Cycle innovations in MGTs

To achieve an optimum efficiency and reduced carbon emissions, variety of modifications have been incorporated in the simple recuperated MGT configuration. The MGTs have been classified into various types based on their fuel flexibility and heat addition mechanisms. The MGT modified cycles are externally fired micro gas turbine (EFmGT),

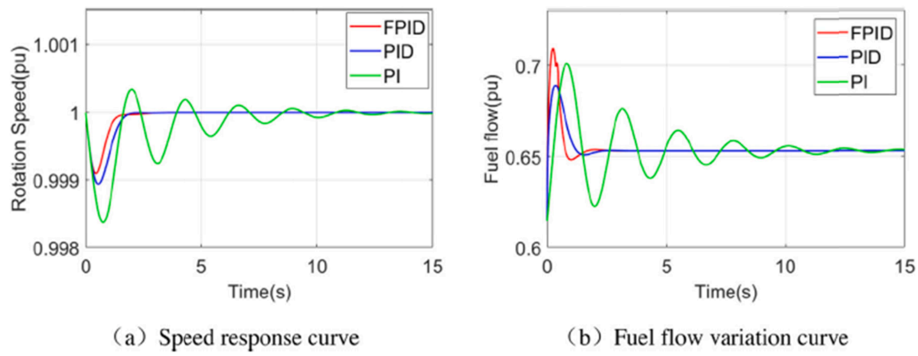

Fig. 14. The response of the output parameters (rotational speed and fuel flow rate) in case of load disturbance, [55].

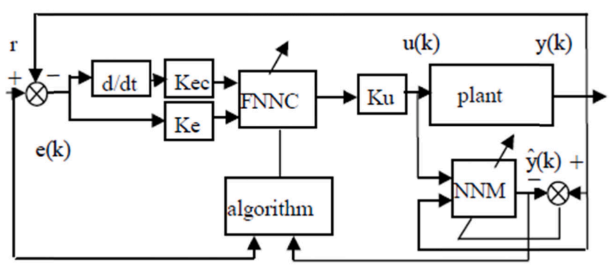

Fig. 15. Schematic of adaptive FNNC, [68].

closed cycle gas turbine (e.g., solar only MGT and solar assisted MGT), and micro humid air gas turbine. The details are mentioned in the following sections.

Externally fired micro gas turbine (EFmGT)

The EFmGT cycle works on the same Brayton cycle as the simple MGT but in the EFmGT the fuel is burned in a separate external combustor. The heat of combustion is transferred to the working fluid i. e., air, through a heat exchanger. Subsequently, this heated air is expanded in the turbine to produce mechanical power [75]. The schematic of an EFmGT is represented in Fig. 19. The EFmGT cycle provides a benefit of burning dirty fuels such as coal and biomass without the need for cleaning and as is needed after gasification process in direct fired MGT. Moreover, the separate combustor is free from the fuel compression and injection accessories. Despite the plethora of existing research, the maximum reported electrical efficiency of a 6 kW open cycle EFmGT powered by natural gas was nearly 24% that is lower than the recuperated MGT [76]. Additionally, the EFmGT needs high temperature burner and heat exchanger that could give a temperature of 1200 K to compete with the power output of a recuperated MGT. Therefore, applied research on high temperature combustor and heat exchanger is underway. EFmGT coupled with a heat recovery unit in CHP applications can provide extra efficiency but with the penalty of additional costly equipment. Moreover, MGT with a dual fuel configuration i.e., an externally fired biomass and an internally fired NG, along with organic Rankine cycle (ORC) bottoming cycle reported an improved efficiency of 29.4% with an energy input ratio of NG (50%) – Biomass (50%) [77]. However, this dual configuration centered study was based on numerical simulations without any experimental implementations. Therefore, there is a room to conduct further experimental

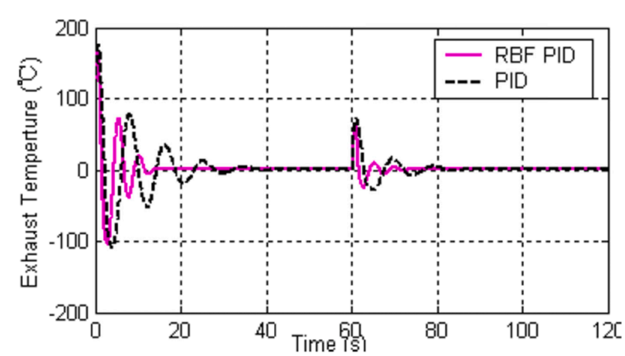

Fig. 17. Comparison of RBF tuned PID with classical PID, [70].

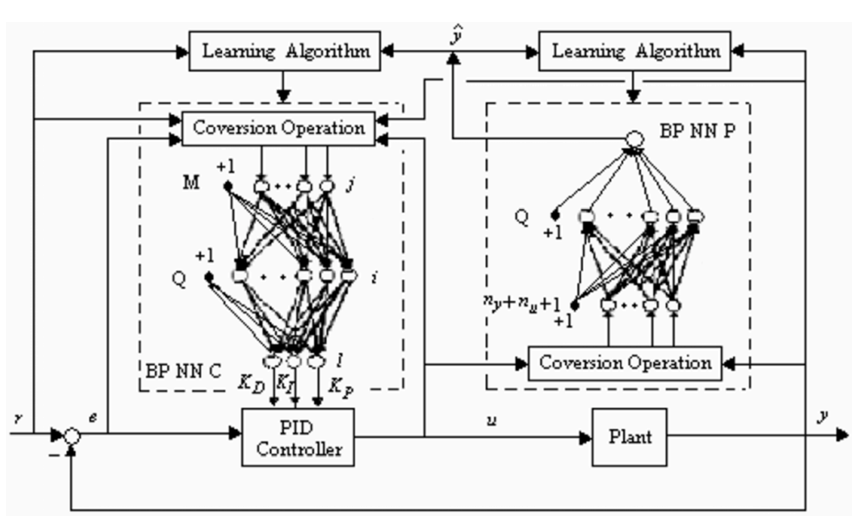

Fig. 16. Adaptive PID controller with BPNN tuning, [69].

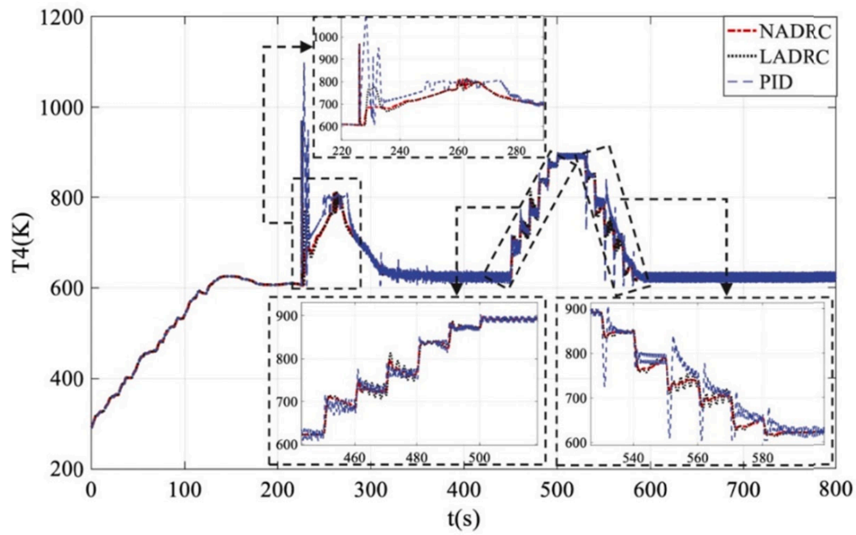

Fig. 18. Comparison of NADRC, LADRC and PID for TOT, [72].

Table 3
Comparative analysis of studies dealing with advanced controllers.

Author	Methodology	Control parameters
Yang et al., [55]	The fuzzy PID controller was tuned with the PSO and cuckoo search algorithm	Temperature and speed
Lin et al., [72]	NADCRC along with nonlinear error state feedback control law and nonlinear observer	Speed, power tracking, NADRC, LADRC and PID comparison
Zaccaria et al., [62]	An observer based adapted MPC controller was developed for a performance degraded MGT	TIT and surge margin
Moustafa and Hassan [66]	PSO and advance accelerated coefficient PSO-based techniques	Temperature, acceleration, and speed
Wu et al., [64]	Data-driven predictive controller using SID method to develop predictor from the data without establishing models	DDPC
Zhu et al., [63]	MPC	Shaft speed, outlet cooling water temperature, and outlet heating water temperature
Shixi et al., [65]	MPC	–
Alizadeh [67]	GA-based optimization of PI coefficients	–
Wei et al., [73]	SPWM using PSCAD software tool	Shaft speed, acceleration, and TOT
Wang et al., [70]	Self-adapted PID controller tuned with RBF neural network	TOT
Wang et al., [69]	self-adaptive PID controller tuned with back propagation neural network	TOT
Deng and Zhang [68]	Fuzzy neural network-based adaptive controller	Shaft speed
Li et al., [74]	Causal ordering graph (COG) method based on nonlinear differential equations	Air mass flow and speed

research by integrating EFmGT with ORC.

The biomass fuel taken from different sources (feedstocks) has distinct features such as heating value, moisture content and external temperature. Therefore, the dynamic performance study of an EFmGT is of crucial importance owing to larger volume of burner, heat exchanger, and varying nature of biomass fuel composition and moisture content. The other typical issues like difference in inertia and dynamic response between turbomachinery (and rotor shaft), and recuperator (and heat

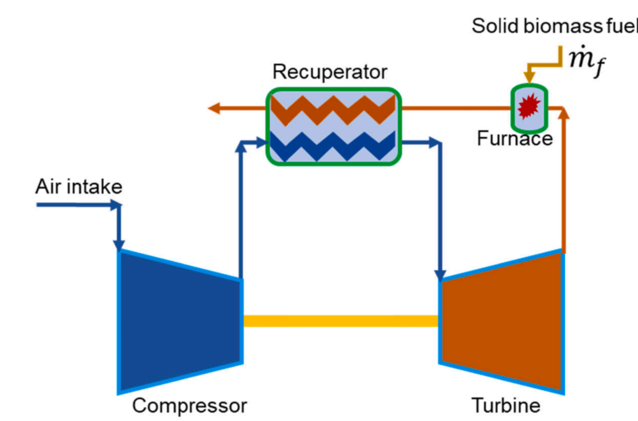

Fig. 19. Schematic of an externally fired micro gas turbine.

exchanger) urge a faster controller for better stability of engine. Traverso et al., [20] utilized the TRANSEO code to simulate the transient performance of EFmGT. The findings of the study revealed that the effect of heat storage on the turbomachinery components was significant during transient operation. Moreover, turbine showed higher oscillations as compared to compressor, and EFmGT was vulnerable to surging of the compressor as well. It was concluded that surging and high pressure oscillations are harmful for heat exchanger owing to larger volumes in EFmGT [20,40]. In another study Traverso et al., [40] investigated the transient performance of a commercially available engine with certain additions such as high temperature recuperator along with an externally fired combustor. The built-in combustor was retained to assist in start-up operations. The experimental study incorporated new control valves, including a notably fast response bypass valve, and a slow response combustor control valve to effectively control the shaft speed and TIT, thereby maintaining a surge free operation. Barsali et al., [36] developed a dynamic simulation model for a 70 kW EFmGT coupled with an ORC to observe the response of fuel change and fuel moisture content in the presence and absence of a controller. It was revealed that the increase in biomass moisture content decreases the TIT and power output of cycle without controller. Using the control strategy averted the already mentioned problem of power change. However, the ORC depicted a delayed response as compared to MGT due to a higher thermal inertia of the ORC system. Al-Attab and Zainal [78] conducted an experimental study to demonstrate the start-up dynamic operation of a self-designed turbocharger-based EFmGT. The engine start-up operation was initiated by using two separate prime movers i.e., two series connected air blowers and a centrifugal air compressor [78]. Both methods failed to reach a self-sustaining mode and start-up could not be proceeded. However, this study could not investigate the effect of dynamic operation on overall efficiency and safety of the EFmGT.

Within the literature, it can be seen that the dynamic performance studies on the EFmGT technology are rare. The lack of market penetration owing to low efficiency also hindered the way for doing further research on this cycle. Among the few studies that considered the dynamic performance of EFmGT only one study considered experimental implementation. To make EFmGT competitive to the counterpart technologies, the numerical and experimental dynamic performance studies of EFmGT associated with ORC are needed for better understanding of the operational flexibility of hybrid systems in distributed energy network.

Solar-based micro gas turbines

The concept of concentrated solar power (CSP)-based Brayton cycle was firstly coined when NASA developed a solar powered MGT to produce electricity for their space applications. The mechanism of power generation through this idea is based on directing the solar irradiance of the concentrator on the receiver. The receiver positioned in the focal point of the concentrator, further absorbs and transforms the solar irradiation into sensible heat of the working fluid that is used by turbomachinery components in a closed or open cycle configuration to produce electricity [79,80]. Normally, two kinds of solar powered MGT configuration are adopted based on a variety of environmental and economic factors. First configuration is the solar only MGT that is solely based on the solar irradiation. The other one is solar assisted MGT (or solar hybrid MGT) that consist of a solar receiver along with an auxiliary combustor for backup support during unavailability of sun [81]. The schematics of both configurations are illustrated in Fig. 20(a and b). The integration of high temperature thermal energy storage (TES) with CSP-MGT provides a viable option for storing the excess solar energy in the daytime and further utilizing the stored energy during cloudy weather or nighttime [82]. TES can be performed in different ways e.g., sensible, latent, and thermochemical energy storage and via different materials including concrete, ceramic, molten salt, and phase change materials (PCMs) [83,84]. The schematic of a TES-based solar hybrid MGT is shown in Fig. 21.

Since the performance of a Brayton cycle is closely tied to the TIT, the CSP-MGT faces a huge challenge in providing a continuous power. The CSP-based MGT is typically dependent on the direct normal irradiance (DNI) that fluctuates with the weather and varying sun position. This varying DNI in turn pushes the MGT to work in off-design and transient conditions. Additionally, solar only MGT shows a delayed dynamic response in the event of sudden load variation due to larger inertia of the concentrated solar dish system. Apart from this, load fluctuation that

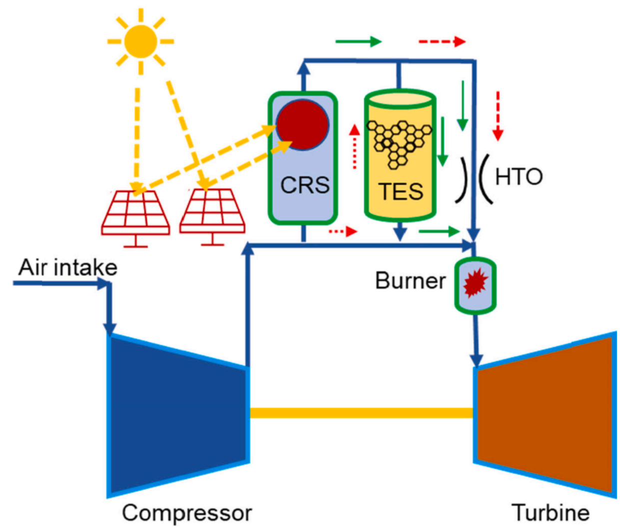

Fig. 21. MGT associated with concentrated solar power and thermal energy storage (CRS is central receiver system, and HTO is high temperature orifice).

proceeds with acceleration or deceleration might be responsible for rotor over speeding or shaft breakage/emergency shutdown, respectively [85]. Similarly, the solar hybrid MGT configuration faces dynamic operation too. For instance, the MGT works on solar-based energy with less combustor fuel flow during solar rich hours, while sudden reduction in DNI urges the MGT to activate the higher fuel flow. Similarly, when the solar irradiance is restored the fuel flow is reduced. This fuel variation leads to flameout phenomenon and dynamic instabilities in the combustor, thus increasing the complexity of the system. Moreover, sudden generator load rejection leads to over speeding of the shaft due to higher volumetric and thermal capacity of a solar hybrid gas turbine system operating in a standalone mode. It was suggested to either install additional relief system (such as a blow-off valve) or increase the rotor inertia to achieve safety of the system [86]. Another research also highlighted the same over speeding issue in a megawatt-scale gas turbine [87]. Hence various dynamic response and control related concerns for a stable and safe operation of MGT are raised in both configurations of the solar-based MGT.

The pertinent literature exists in the domain of dynamic performance study of solar-based gas turbines for megawatt scale power generation through the solar hybrid combined cycle units as reported by Traverso et al., [82]. However, dynamic performance and control studies of solar only MGT are found to be scarce up to authors knowledge. Ghavami et al., [88] compared two different operation and control strategies i.e., maximum permissible power (MPP) and novel recuperation control of solar only MGT for the OMSoP project. These control strategies are

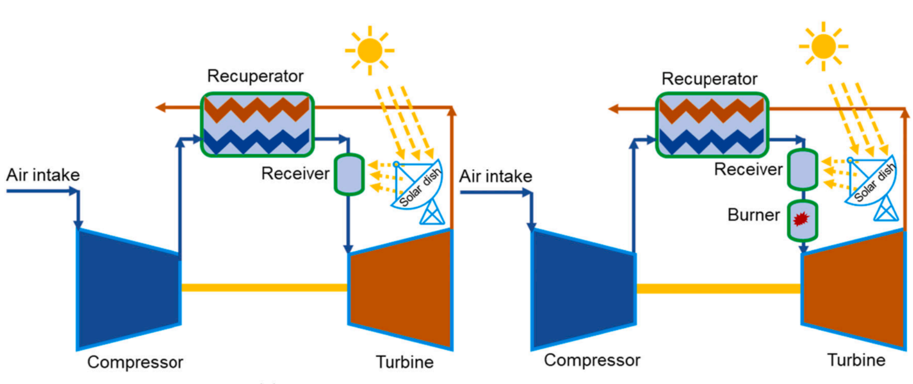

Fig. 20. (a) Solar only MGT, versus (b) solar-assisted MGT.

helpful for maintaining a wide power and efficiency envelop along with safety for load-independent and load-dependent solar only MGT. Although the recuperation control strategy needs additional expense for installing new valves, it offers greater control flexibility over MPP. The grid/load independency challenges of the CSP-MGT can be countered by integrating a TES system. Although TES provides the added benefit of short-term energy storage, it also leads to compressor surging and pressure drop changes due to frequent charging and discharging of TES. Hence, Barberis et al., [89] examined the dynamic performance of a 100 kW solar hybrid MGT integrated with a ceramic honeycomb-based high temperature TES system using the TRANSEO code. In another study, the modified system installed 3 three-way valves on cold side to avoid the expense of hot side valves along with heat exchanger [90]. It was revealed that pressure drops, and thermal gradient were predicted accurately during cold conditions. However, the results were not satisfactory during hot conditions because the 1-D discretization assumptions of the TRANSEO code could not capture the real-time radial interaction with the metallic vessel. This issue was further investigated in a study by Mahmood et al., [91] that compared the dynamic performance of 1-D TRANSEO and 2-D CFD models and validated the results with the experimental test rig data. The study reported that the CFD model predicted the thermal behavior of TES accurately at the cost of computational expense while 1-D model showed deviation from experimental results. It was concluded that the TRANSEO tool could be applied for initial design phase and sensitivity analysis of TES-based CSP-MGT energy systems. The more recent study by Chen et al., [92] developed a dynamic model of solar hybrid MGT integrated with TES during load and DNI changes. During load reduction of more than 18 kW, the position adjustment of solar heliostat away from receiver was proposed to avoid failure risks of components. In case of load increase greater than 25 kW, stepwise load increase was suggested for safety purposes. The effect of load change on different performance and safety parameters have been illustrated in Fig. 22.

Micro humid air turbines (mHATs)

Despite the advantages of lower emissions, reduced maintenance and quieter operation of MGT technology, it has lower efficiency as compared to its competitive technology, i.e., internal combustion engines (ICE) [93]. The MGT technology has inherently been built for CHP applications giving an overall cycle efficiency of around 80% (electrical: 30%, thermal: 50%). However, in the period of low or no heat demand especially in summer, this technology manifests a reduced efficiency (30%) because of waste of the generated heat. This situation renders less net present value (NPV) because of shutdown in the summer period [94]. Owing to this reason, several studies have been conducted to increase efficiency of MGT by increasing turbomachinery components efficiencies along with recuperator efficiency enhancement. The most pragmatic idea in this regard is to modify the existing MGT cycle by integrating humidification process. In this regard, the exhaust heat is typically utilized in an economizer to further produce steam or hot water. Subsequently, this steam or hot water is injected downstream of the compressor increasing the mass flow of the working fluid and resulting in an increased specific power of the turbine, while keeping the compressor work unchanged. This results in a higher electrical efficiency of the MGT unit. The cycle developed in this humidification configuration is known as micro humid air turbine (mHAT) cycle. A schematics of three different water and steam injection-based cycle layouts are shown in Fig. 23.

It has been revealed in an experimental study conducted by Carrero et al., [96] that water injection helped in gaining both power and electrical efficiency by more than 30% and 4.2% respectively, as compared to that of a dry cycle. De Paepe et al., [95] have reviewed and elaborated several advantages and critical aspects of various water and steam injection layouts in mHAT cycles. Apart from the advantages of

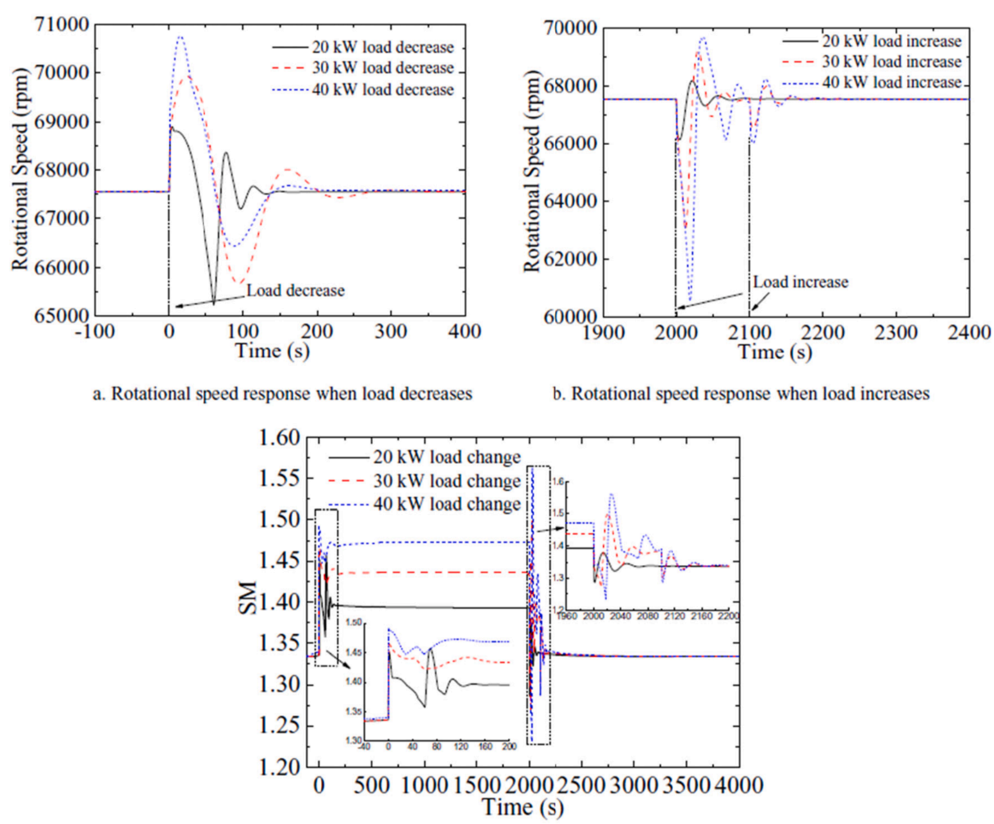

a. Rotational speed response when load decreases
b. Rotational speed response when load increases
c. Surge margin response

Fig. 22. Effects of load changes on performance parameters of solar hybrid MGT, [92].

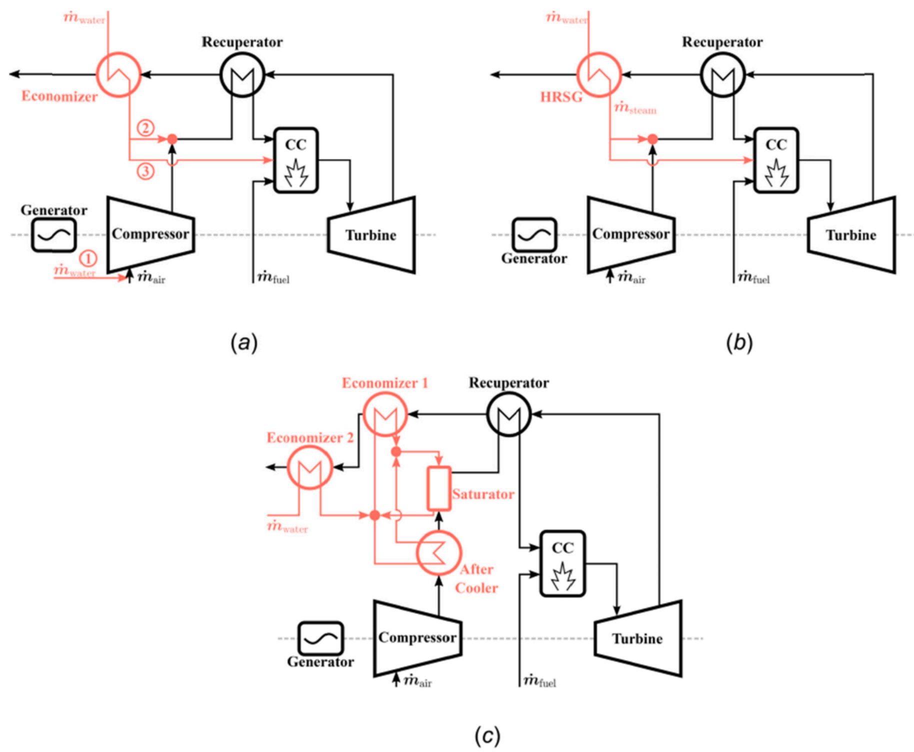

Fig. 23. The possible wet cycle layouts, (a) water injection in compressor, (b) steam injection in burner, and (c) water injection using saturation tower and water recovery mechanism, [95].

the humidification, a few constraints have been noticed through experimental studies. For instance, integration of saturation tower and associated extra piping system gives rise to pressure losses in the cycle that could decrease the surge margin in the compressor. The bleed air concept can be utilized to alleviate surging but at the expense of the performance deterioration. Moreover, pressure loss can trigger the control system to exceed the shaft speed beyond the design point rotational speed, to fulfill the constant shaft power demand. Furthermore, the water addition along with high temperature exhaust gasses can negatively impact the life of the recuperator by depleting the chromium content in the stainless-steel material especially on the hot side of the recuperator. The humidification leads to imbalance between the compressor and turbine mass flow that might create shaft mechanical stresses and axial thrust causing rotor instabilities. The complications arising with the addition of humidification tower emphasize the need to develop numerical and experimental dynamic studies (especially at start-up and shutdown) for mHAT cycles to ensure operation flexibility and safety.

The transient/dynamic performance studies corresponding to mHAT have been conducted quite scarcely. The initial studies in this regard were focused on developing a start-up operation strategy for better performance of the humidified cycle. Hence, two start-up strategies, i.e.,

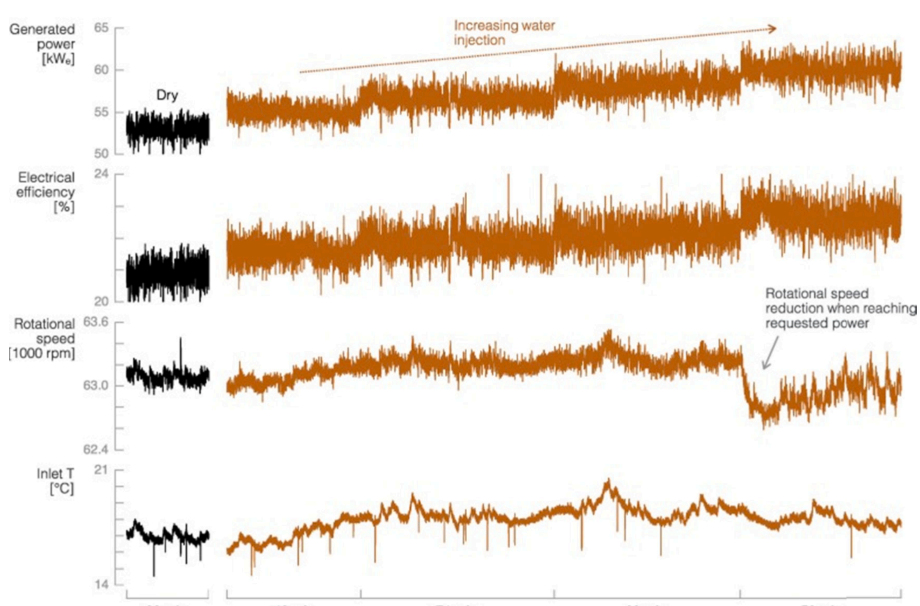

Fig. 24. Effect of increasing water injection on different parameters at a constant power demand, [96].

wet, and dry strategies were experimentally tested. The preliminary studies showed a flameout condition and subsequent surging in the compressor during both wet and dry start-up operation [97]. The probable reason was reported to be the constrained energy transfer in the saturator in the experiments. However, in the follow up experiments surging mitigation using bleed valve led to a stable start-up operation for two different periods of time i.e., 3 and 1.5 h [98]. A comparison of wet and dry cycles corresponding to various parameters was conducted at the constant power of 60 kW, as shown in Fig. 24. The sequential increase in steam injection increases the power output and the electrical efficiency. However, the shaft speed seems constant because the maximum limit of speed is achieved before reaching a required power setting owing to pressure losses and bleed air effect.

The experimental campaigns have shown that the water injection leads to a reduced surge margin (by ~9%) typically in the power setting range of 59.7–68.9 kW. In this regards, a transient model based on the TRANSEO code was developed by Carrero et al., [37] that particularly focused on the effect of power step ramp on the oscillations and surging. To ensure a stable operation, a maximum limit for load increase and decrease ramp rates were observed. Fig. 25(a), illustrates the increased power ramp settings of 2, 4.2, and 16 kW/s. The higher power ramp showed a significant reduction in the surge margin. Among the decreased power ramp settings of –1, –3.5, and –25 kW/s, the highest ramp rate (–25 kW/s) does not decrease the surge margin as much as in other settings. Therefore, it was shown that higher ramp rates (i.e., 16 kW/s) in case of power increase are more vulnerable to surge as compared to higher ramp rates in decreased power settings, as shown in Fig. 25(b). The tests were planned to keep the ramp rate for both cases up to 2 kW/s to avoid instability in the compressor. Since the saturator temperature is the most significant parameter in a mHAT, the effects of saturator inlet temperature control on the steady state and dynamic performances of mHAT were studied by Huang et al., [99]. The results showed that the saturator temperature control had a very little effect on the power output changes, while it helped in achieving a faster stability in the saturator component.

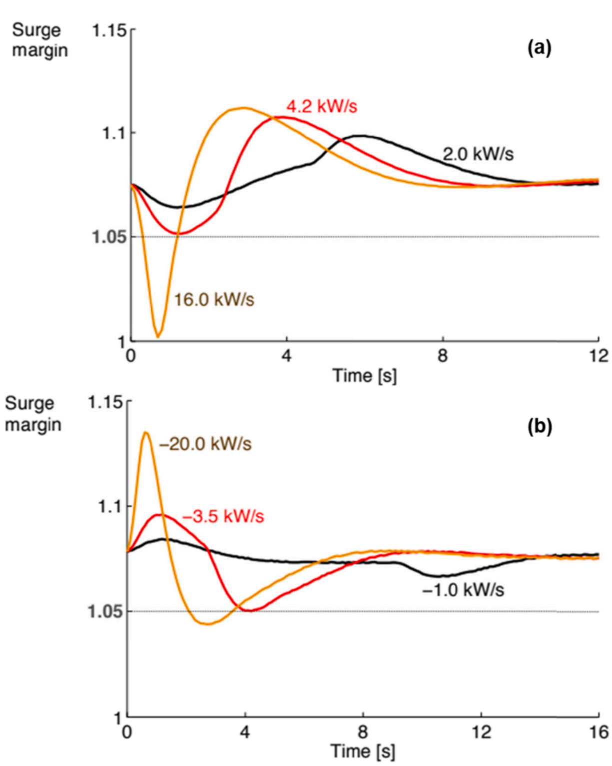

Fig. 25. Dynamic ramp rates, (a) increased ramp in power, (b) decreased ramp in power, [37].

SOFC–MGT hybrid systems

Solid oxide fuel cell is a proven clean, quiet, and efficient stationary power technology finding suitability in a wide range of applications such as households, commercial and transport sectors. In today's scenario of global sustainability expedition, SOFC have a huge potential to be integrated with renewable (e.g., solar PV and wind) and conventional energy technologies (e.g., gas turbines, steam turbines, and internal combustion engine). The particular reason for hybridization of MGT and SOFC lies in the fact that the hybrid system with gas turbines gives an increased efficiency up to ~70% that is far beyond the efficiencies of independent systems (i.e., gas turbine: ~35%, SOFC: ~50%) [100]. Moreover, integration of SOFC with MGT in hybrid mode is a promising option owing to considerably high exhaust temperature (greater than 500°C) that substantiates the utilization of high grade heat for further electricity generation [101]. In addition, the compatibility of the exhaust gas temperature of SOFC with TIT of the MGT synergizes the need for hybridization [102]. Regardless of the promising features of this hybrid technology, it could barely reach the commercialization owing to unavoidable controller problems according to authors' best knowledge.

Among variety of hybridization options, MGT has only been experimentally established and tested so far in the literature. Among the leading organizations and institutions involved in the research and development pertinent to hybrid SOFC–MGT are U.S., Department of Energy (DOE) [103], National Fuel Cell Research Center (NFCRC) at University of California, Irvine [104], and Mitsubishi Heavy Industries in Tokyo Gas Senju Techno Station [105]. Besides full experimental test rigs, variety of hybrid SOFC–MGT emulators have been designed and developed that consist of real MGT coupled with a fuel cell simulator in form of a larger volume. The combination of hardware and software in this manner is normally known as cyber-physical systems. For instance, Thermochemical Power Group (TPG) in their laboratory at the University of Genoa, Italy [106], German Aerospace Center (DLR), and National Energy Technology Laboratory (NETL), at the U.S. DOE, developed and operated the emulators to better perceive the hybrid system's dynamics, integration and control challenges without risking the damage of the expensive and delicate components via experimentations. Several configurations of SOFC–MGT have been designed by many researchers to optimize the electrical efficiency and capital costs [107,108]. The commercially available MGT ranging from 30 kW to 100 kW capacity have been widely integrated with SOFC in the open literature. One simplistic layout of the hybrid system is illustrated in Fig. 26. The compressor normally pressurizes the intake air up to the fuel cell's operating pressure. The compressed air is firstly passed through the recuperator; enters the cathode side of the stack and hence partakes in the electrochemical process. Whereas the anode side receives the preheated and compressed fuel to be initially reformed and subsequently

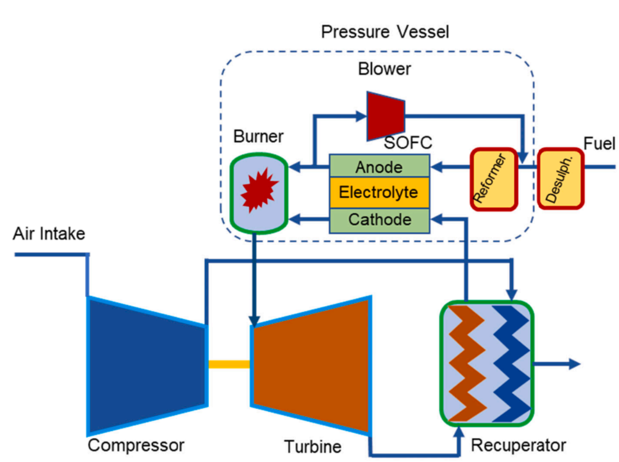

Fig. 26. Schematic of an SOFC–MGT hybrid system.

contributes to the reaction process for electricity generation. The synergy is achieved by burning the remaining untreated fuel and exhaust air from the cathode in the downstream combustor, and eventually high temperature flue gases are expanded in the turbine section for mechanical shaft power [109].

Part-load and transient scenario. The hybrid SOFC–MGT are normally operated in two modes i.e., standalone or integrated with RES for distributed power generation. In a standalone mode, the off-design and part-load operations are faced to meet the load demand [110]. Similarly, in a RES-integrated mode, several transient phenomena (e.g., start-up, load change and shutdown) are likely to occur due to fluctuating nature of the solar PV or wind. Additionally, the temperature gradients in high temperature SOFC can also lead to unavoidable transients. In this regard, the system undergoes complex non-linear dynamics. The frequent load transitioning raises significant concerns over control system, safety, and reliability of the hybrid system. To counter these operational safety issues, safe operation zone is demarcated on the performance maps to identify the unsafe and critical operating limits. To this end, a failure free operation is achieved by constraining various parameters such as thermal runaway (maximum and minimum allowable temperature limits), thermal fatigue, thermal cracking, carbon accumulation, compressor surging, and over speeding. In this context, the study of transient performance of hybrid SOFC–MGT systems becomes indispensable. Fig. 27 demonstrates an allowable limit of various operating parameters along with safe operating region on performance maps.

The hybrid MGT–SOFC integrated with variable RES need to cope sharp and rapid load variations to maintain the grid resilience. The existing literature in the domain of dynamic performance studies of hybrid SOFC–MGT system is segregated in dynamic system analyses and experimental test facilities-based studies. In system analyses studies, majority of the investigators incorporated the rapid load changes up to ~66% in time frame of tens of hours [112–116]. Whereas in experimental test facilities, the researchers could accomplish load transition merely up to ~20% while operating in a time window of minutes to hours [117,118]. Different load change strategies as a function of transient operating time window are depicted in Fig. 28. However, a load transition up to 50% in operating window as short as seconds is inevitable to accommodate the drastic intermittency of RES. In this regard, a recent study by Zhang et al., [119] considered a novel approach

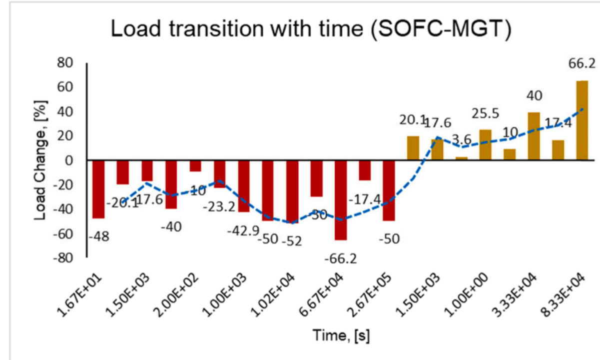

Fig. 28. Various load change strategies in the existing literature.

by coupling a cyber-physical system consisting of hybrid SOFC–MGT system with a grid simulator that is capable of a rapid load variation up to ~50% in a window of 10 s. The schematic of a novel cyber-physical system is illustrated in Fig. 29.

Control strategies. The inherent purpose of the control system in hybrid SOFC–MGT is to monitor and avoid several risk situations associated with performance and safety of the hybrid system. The notable parameters comprise of unwarranted temperature in SOFC, unwarranted pressure difference between cathodic and anodic sections, extremely modest steam to carbon ratio in the reformer of SOFC, the MGT's rotor over speeding, compressor surging, and unnecessary thermal stress in the heat exchanger of SOFC. These critical parameters need to be monitored and controlled during start-up, shutdown, and rapid load transition. However, developing a control system poses a biggest challenge due to considerably different transient time scale associated with two distinct energy systems i.e., SOFC and MGT [120]. The extremely diversified higher thermal inertia of SOFC and lower shaft inertia of MGT require tailored controlled strategies that could avert the over speeding and other unstable operations.

A detailed literature review reveals that plenty of studies exist in literature regarding the dynamic operation and control of SOFC–MGT systems. Most of the studies have focused on designing control strategies for turbomachinery running at constant shaft speeds. However, the variable speed in turbine might cause degradation in the stack because

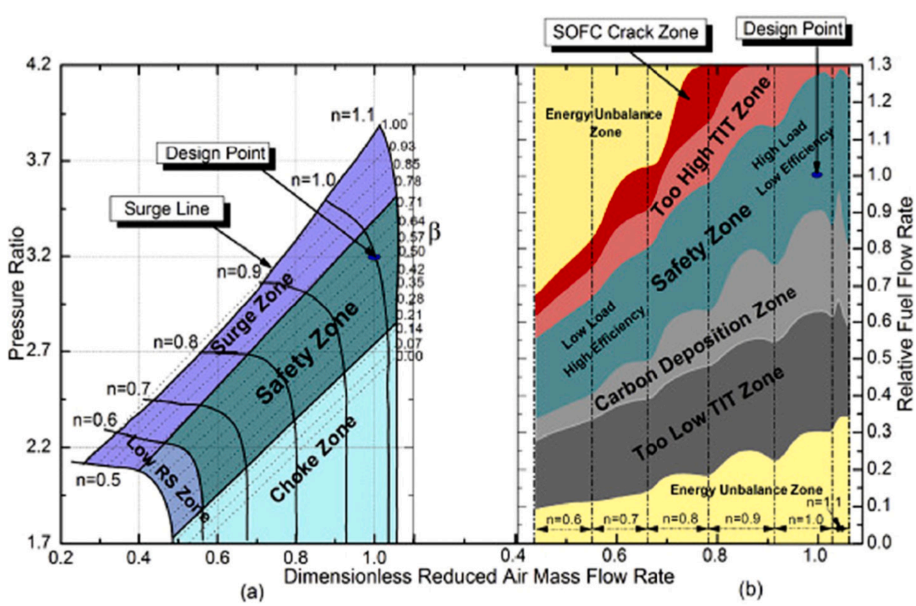

Fig. 27. Operation zones for a hybrid SOFC–MGT, [111].

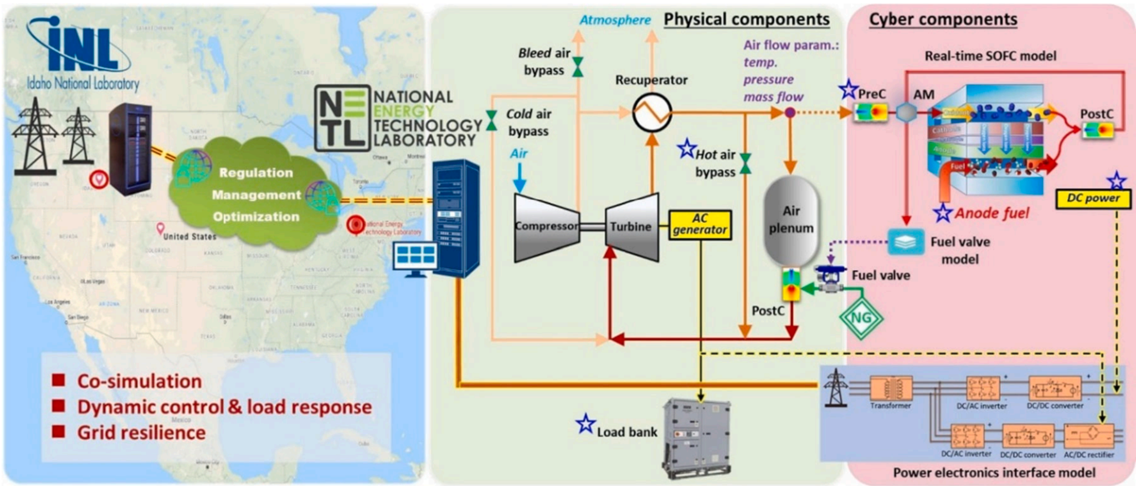

Fig. 29. A novel cyber-physical SOFC–MGT associated with grid simulation, [119].

of pressure fluctuations. Hence, there is a need to develop advanced control schemes for variable speed operations of turbines. Though the literature is rich in transient simulation-based studies, is shallow in experimental studies. Therefore, the experimental prototypes based on transient performance studies are of crucial importance for commercialization of the technology. In addition to this, the literature lacks such kind of control strategies that could prevent the several degradation mechanisms i.e., thermal gradients and transients, as well as compressor surging and stalling.

Dynamics of alternative fuel utilization

Influence of burning 100% hydrogen fuel

Gas turbine industry is ambitious to manufacture gas turbines that can work on 100% hydrogen fuel by 2030, thereby ensuring a CO_2 neutral gas fired power generation [121]. To the date, MGT available in the market are capable of separate burning of natural gas (NG), biogas, and syngas. Apart from separate burning, the other option is burning blends of renewable fuels such as syngas and hydrogen with natural gas in existing NG-fired MGTs. The blending concept currently lacks maturity and can incorporate hydrogen percentages only up to 20% (vol.). The main challenge in employing hydrogen in a MGT is its different combustion behavior as compared to natural gas. Owing to significant differences in flame speed and Wobbe index (WI) of hydrogen and natural gas, a typical combustor configured for NG cannot handle the hydrogen content beyond a certain limit. The other challenges that hydrogen can pose are the flashback and thermoacoustic instabilities during the start-up and shutdown operations. For instance, the volumetric LHV of hydrogen (10.8 MJ/Nm^3) is lower and roughly accounts for one-third of methane (35.8 MJ/Nm^3). Therefore, to operate a MGT on hydrogen, almost three times more volumetric flow rate (than NG) will be needed to produce the same amount of power [122]. Given these challenges, dedicated combustors are needed to be developed for 100% combustion of hydrogen. Nevertheless, the research and development pertinent to burning different fuel blends is underway.

Blending of hydrogen with natural gas (H_2NG)

The fuel blending scenario can incorporate up to 5–10% (vol.) hydrogen in existing NG combustor with little to no modification in the system. To cater higher volumetric flow rate of hydrogen, modified fuel piping and fuel injectors are needed. However, for greater percentages of hydrogen (i.e., more than 15% (vol.), a substantial retrofitting of the MGT components will be needed such as reconfiguration of the entire combustor. Moreover, for blending hydrogen with the existing NG infrastructure, a fuel blending system needs to be devised that could properly mix the hydrogen in the existing fuel with greater control. A dynamic model was developed by Gaeta et al., [31] for a 100 kW MGT hybridized with solar PV that produces green hydrogen via water electrolysis. The effect of dynamic triggers such as ambient temperature, fuel composition variation, and load variation were investigated in the model. It was reported that the MGT running on NG and 10% (vol.) hydrogen blends showed promising results by compensating the power fluctuations from intermittent energy sources along with significant CO_2 reductions. The partial hybridization of the systems reported a fuel economy of up to 37.5% and full hybridization accounted for a fuel economy of 41.5%. To accommodate the variety of high-pressure fuel blends with hydrogen, new decompression and distribution units were designed. Moreover, two digital thermal mass flow meters were installed to measure the fuel blends' mass flow rate coming from the main and pilot fuel lines to the combustor. Similarly, a 100 kW capacity MGT was recently retrofitted with a new FLOX burner at the University of Stavanger, Norway [123]. The experiments led to an MGT running on 100% hydrogen. Moreover, the newly retrofitted test facility has the flexibility of burning the variety of renewable fuels. However, dynamic performance studies based on various blends of hydrogen with NG and other renewable fuels are under progress.

Low calorific value fuels (biogas and syngas) in MGTs

In addition to green hydrogen, low calorific value (LCV) fuels such as syngas has gained momentum in energy transition. An experimental and numerical study conducted by Zornek et al., [124] revealed that a LCV fuel namely biogas obtained from anaerobic digester and thermal gasifier had a huge prospect in decreasing the NO_x and unburned hydrocarbons (UHC). Moreover, MGT operating with low LHV fuel in a FLOX combustor has increased fuel flow rate that reduces the air mass flow of the compressor. Hence, compressor takes less mechanical power for compression that in turn increase the overall mechanical power of the engine. It was also revealed that the biogas improved the surge margin as compared to the natural gas. Due to combustor reconfiguration, new fuel mass flow meters were installed to regulate pilot fuel along with a modified pre-set fuel map and pressure independent adjustable fuel nozzle. Similarly, Nikpey et al., [125] conducted an experimental study to evaluate the effect of burning mixture of biogas and NG on MGT performance and emissions. A dedicated gas mixing station was installed for proper mixing of different fuel mixtures. The study revealed that biogas and NG mixtures did not affect the engine efficiency and safety substantially; however, carbon emissions could be reduced without any modification to the hardware of the engine.

Apart from the H_2NG blends, the literature consists of some studies considering the fuel blending of various biomass gasification products (biogas, syngas) and NG. Similarly, De Santoli et al., [126] conducted a study to investigate the influence of summer and winter ambient conditions on the performance and emissions of an MGT. The fuel blends of NG with 10% (vol.) hydrogen were tested for a period of one year. It was revealed that hydrogen addition can compensate the performance deterioration caused by ambient conditions in summer, while in winter there was no substantial gain in power due to hydrogen enrichment. Moreover, hydrogen enrichment penalizes the efficiency at part-load during winter. The NO_x emissions were observed to be increased, while carbon emissions were decreased significantly in blending mode. Recently, Gholamian et al., [127] used the TRNSYS tool to develop a dynamic simulation of two MGTs of 200 kW and 65 kW capacities integrated with a polymer electrolyte membrane (PEM) electrolyser. The MGTs in this study had been reported to be utilizing blends of hydrogen and biogas to fulfil the electricity and heat demands of a wastewater treatment plant. The study revealed that utilizing hydrogen led to reduction in CO_2 emissions by 30%. In addition to the dynamic simulation, the study conducted a techno-economic analysis of the simulated plant configuration. The levelized cost of hydrogen (LCOH) was reported to be significantly lower than the base-case scenario, while the payback period was estimated to be 6.5 years.

New techniques such as water and steam injections have been proposed to improve the performance and emissions of MGTs working on alternative fuels. Recently, Renzi et al., [128] performed a numerical study for 100 kW MGT fueled with syngas. The steam injection was adopted to enhance the electrical efficiency and emission reduction. It was concluded that syngas can be burnt in the MGT with reduced efficiency and increased emissions; however, the steam injection cycle has the flexibility in tailoring the cycle for electrical and thermal requirements along with an enhanced performance. Similarly, Reale et al., [129] conducted a numerical study to investigate the effect of steam and water injection on thermodynamic performance of compound humid air turbine – steam injection (HAT–STIG) cycle burning hydrogen enriched methane. It was revealed that steam injection in the combustor is more suitable as compared to water injection before the saturator in the HAT cycle. Both techniques have their own respective benefits; HAT cycle gives enhanced power and efficiency, while the STIG cycle gives enhanced percentages of hydrogen enrichment. In depth literature search manifests that the commercialization of both HAT and STIG could not be achieved so far.

A detailed literature review of the alternative fuel debunked that the current literature is pale in dynamic performance studies of alternative fuel based MGTs. The existing literature only considers blending hydrogen up to 20% (vol.) for reduced emissions. However, this small amount of hydrogen enrichment cannot contribute in decarbonization, substantially. The research work is in progress to replace the existing NG combustor with the dedicated H_2-based combustors for 100% transition to cleaner future. Moreover, experimental, and numerical research with enhanced hydrogen enrichment (greater than 20% (vol.)) is needed in future.

Conclusion and future recommendations

The present review was organized with a view to establish a detailed document consisting of dynamic performance studies along with various control strategies for MGTs. The state-of-the-art in the paper demonstrates several dynamic operating regimes associated with MGTs. A detailed elaboration of dynamic modeling techniques for all the constituent components has been summarized for further research in this domain. The critical analysis performed for this study helped in identifying the research gaps and developing a comprehensive supporting document for future dynamic modeling activities, and subsequent fault diagnosis and prognosis of MGTs. Since dynamic operation is closely tied to the controller design, various classical and advanced control strategies aiming for better performance and safety of the MGT have been critically reviewed. Eventually, prospects and challenges of using alternative fuels (hydrogen and other renewable fuels) in MGTs from a dynamic operation perspective have been presented. The major findings and research gaps of the critical review are as follow:

- The load change dynamic regime especially shifting from full-load to part-load typically alters the operating characteristics in a stand-alone mode, while most of the existing literature has considered only a grid connected mode.
- Majority of the existing literature is based on numerical studies, while a few researchers have considered the experimental performance studies to evaluate the transient performance of natural gas fueled MGTs.
- After an in-depth review of the literature, it became evident that start-up and shutdown transient regimes are likely to be responsible for various engine failures and emergency shutdowns, including causing surging in the compressor and bearings damage due to excessive heat.
- In transient events, the combustor and recuperator have been indicated as the highly critical components in terms of delayed dynamic response due to thermal inertia of metal matrix during external perturbations.
- Physics-based dynamic modeling approaches in the literature are largely based on a lumped volume approach to consider the fluid inertia; however, thermal inertia has been accounted for by a few studies using conjugated heat transfer modeling.
- Most of the dynamic studies of MGTs have incorporated classical controllers such as PI and PID. However, AI-based advanced controllers i.e., FPID controller gives robust stability and control performance during frequent start-ups and shutdowns.
- The enhanced complexity of innovative cycles such as mHAT, SOFC–MGT and solar-based MGT increase the concerns for a robust controller design along with transient performance studies.
- The numerical and experimental dynamic performance studies of integrated MGT cycles with modern bottoming cycles such as ORC and supercritical CO_2 Brayton cycle have been barely accounted for; hence, provides a potential future research horizon.
- The existing literature has mainly considered the dynamic modeling of NG-fired MGTs. The research and development pertinent to burning alternative fuels (hydrogen, methanol, ammonia, biomethane, syngas and blends) in this regard is scarce. The few studies that considered fuel blends of H_2NG employed merely up to 20% (vol.) of hydrogen. However, dynamic modeling of 100% hydrogen and H_2NG blends with higher percentage of hydrogen are of paramount importance for transition to 100% carbon neutral power generation.

Declaration of Competing Interest

The authors declare that they have no known competing financial interests or personal relationships that could have appeared to influence the work reported in this paper.

Data availability

No data was used for the research described in the article.

Acknowledgements

The authors would like to thank University of Stavanger for providing invaluable support in conducting research.

References

[1] IEA, *Energy Technology Perspectives 2020*. 2020, Rep., Int. Energy Agency Paris.
[2] UNFCCC. *The Paris Climate Agreement*. 2015 [cited 2023 27-02-2023]; Available from: https://unfccc.int/process-and-meetings/the-paris-agreement.
[3] Global, E., *Micro Gas Turbine Technology: Research and Development for European Collaboration*. 2017.
[4] Ancona MA, Bianchi M, Branchini L, Catena F, De Pascale A, Melino F, et al. Renewables exploitation via hydrogen production in gas turbine test facilities: the ZEHTC Project. E3S Web Conf 2021;238:02006.
[5] Farhat H, Salvini C. New lifing criterion for land-based gas turbines in flexible operation mode. Energy Rep 2022;8:379–85.
[6] Kim, J., et al. Dynamic simulation of full start-up procedure of heavy duty gas turbines. in ASME Turbo Expo 2001: Power for Land, Sea, and Air. 2001. American Society of Mechanical Engineers.
[7] Seo JM, Park JY, Choi BS. Start-up and self-sustain test of 500 W ultra-micro gas turbine generator. J Phys: Conf Ser 2013;476:012060.
[8] Guan J, et al. Experimental and numerical study on self-sustaining performance of a 30-kW micro gas turbine generator system during startup process. Energy 2021;236:121468.
[9] Sekar, T.C., et al., Starting Characteristics of a Micro Gas Turbine Engine at Different Loading Conditions, in Sustainable Development for Energy, Power, and Propulsion. 2021, Springer. p. 415-436.
[10] Traverso A. *TRANSEO code for the dynamic performance simulation of micro gas turbine cycles*. in *Turbo Expo: Power for Land*. Sea, and Air 2005.
[11] Bracco S, Delfino F. A mathematical model for the dynamic simulation of low size cogeneration gas turbines within smart microgrids. Energy 2017;119:710–23.
[12] Duan J, Fan S, An Q, Sun Li, Wang G. A comparison of micro gas turbine operation modes for optimal efficiency based on a nonlinear model. Energy 2017; 134:400–11.
[13] Duan J, Sun Li, Wang G, Wu F. Nonlinear modeling of regenerative cycle micro gas turbine. Energy 2015;91:168–75.
[14] Srikanth K, et al. Matlab/simulink based dynamic modeling of microturbine generator for grid and islanding modes of operation. Int J Power Syst 2016;1:1–6.
[15] Bozza, F. and R. Tuccillo. Transient operation analysis of a cogenerating micro-gas turbine. in Engineering Systems Design and Analysis. 2004.
[16] Fawke A, Saravanamuttoo H. Digital computer methods for prediction of gas turbine dynamic response. SAE Trans 1971:1805–13.
[17] Sellers, J.F. and C.J. Daniele, *DYNGEN: A program for calculating steady-state and transient performance of turbojet and turbofan engines*. 1975.
[18] Korakianitis, T., J. Hochstein, and D. Zou. *Prediction of the transient thermodynamic response of a closed-cycle regenerative gas turbine*. in *Turbo Expo: Power for Land, Sea, and Air*. 1993. American Society of Mechanical Engineers.
[19] Kim J, Kim T, Ro S. Analysis of the dynamic behaviour of regenerative gas turbines. Proceedings of the Institution of Mechanical Engineers, Part A: Journal of Power and Energy 2001;215(3):339–46.
[20] Traverso, A., F. Calzolari, and A. Massardo. Transient analysis of and control system for advanced cycles based on micro gas turbine technology. in Turbo Expo: Power for Land, Sea, and Air. 2003.
[21] Gambarotta, A. and I. Vaja. A Real Time Dynamic Model of a Micro-Gas Turbine CHP System With Regeneration. in ASME Power Conference. 2007.
[22] Chiang, H.-W.D., et al. An investigation of steady and dynamic performance of a small turbojet engine. in Turbo Expo: Power for Land, Sea, and Air. 2002.
[23] Gaitanis A, Contino F, De Paepe W. Real Time Micro Gas Turbines Performance Assessment Tool: Comprehensive Transient Behavior Prediction With Computationally Effective Techniques. J Eng Gas Turbines Power 2023;145(3): 031006.
[24] Banihabib, R. and M. Assadi. *Dynamic Modelling and Simulation of a 100 kW Micro Gas Turbine Running With Blended Methane/Hydrogen Fuel*. in *Turbo Expo: Power for Land, Sea, and Air*. 2022. American Society of Mechanical Engineers.
[25] Raggio, M., D. Bellotti, and M.L. Ferrari. *Transient Analysis of a Micro Gas Turbine With Fuel Composition Change*. in *Turbo Expo: Power for Land, Sea, and Air*. 2022. American Society of Mechanical Engineers.
[26] He, T., et al., *START UP AND SHUT DOWN SIMULATION OF MICRO GAS TURBINE BASED ON REINFORCEMENT LEARNING*. 2019.
[27] Henke M, Monz T, Aigner M. Introduction of a new numerical simulation tool to analyze micro gas turbine cycle dynamics. J Eng Gas Turbines Power 2017;139 (4).
[28] Gaitanis A, et al. Towards Real Time Transient mGT Performance Assessment: Effective Prediction Using Accurate Component Modelling Techniques. Proceedings of Global Power and Propulsion Society 2022:8.
[29] Amelio M, et al. Dynamic simulation of the temperature inlet turbine control system for an unfired micro gas turbine in a concentrating solar tower. Energy Procedia 2018;148:712–9.
[30] Xu X, et al. Data-driven dynamic modeling of coupled thermal and electric outputs of microturbines. IEEE Trans Smart Grid 2016;9(2):1387–96.
[31] Di Gaeta A, et al. A dynamic model of a 100 kW micro gas turbine fuelled with natural gas and hydrogen blends and its application in a hybrid energy grid. Energy 2017;129:299–320.
[32] Seo J, et al. Development and experimental investigation of a 500-W class ultra-micro gas turbine power generator. Energy 2017;124:9–18.
[33] Singh V, Axelsson L-U, Visser W. Transient Performance Analysis of an Industrial Gas Turbine Operating on Low-Calorific Fuels. J Eng Gas Turbines Power 2017; 139(5):051401.
[34] Kim MJ, Kim JH, Kim TS. Program development and simulation of dynamic operation of micro gas turbines. Appl Therm Eng 2016;108:122–30.
[35] Tisarev, A., et al. *Natural Cooling Affecting the Restart of Micro Gas Turbine*. in *Turbo Expo: Power for Land, Sea, and Air*. 2016. American Society of Mechanical Engineers.
[36] Barsali S, et al. Dynamic modelling of biomass power plant using micro gas turbine. Renew Energy 2015;80:806–18.
[37] Montero Carrero, M., et al. *Transient simulations of a T100 micro gas turbine converted into a micro humid air turbine*. in *Turbo Expo: Power for Land, Sea, and Air*. 2015. American Society of Mechanical Engineers.
[38] Shankar G, Mukherjee V. Load-following performance analysis of a microturbine for islanded and grid connected operation. Int J Electr Power Energy Syst 2014; 55:704–13.
[39] Hosseinalipour S, Abdolahi E, Razaghi M. Static and dynamic mathematical modeling of a micro gas turbine. J Mech 2013;29(2):327–35.
[40] Traverso A, Scarpellini R, Massardo A. *Experimental results and transient model validation of an externally fired micro gas turbine*. in *Turbo Expo: Power for Land*. Sea, and Air 2005.
[41] Davis Jr, M., et al. *Joint Dynamic Airbreathing Propulsion Simulations Partnerships (JDAPS)*. in *Turbo Expo: Power for Land, Sea, and Air*. 1995. American Society of Mechanical Engineers.
[42] da Cunha Alves MA, Barbosa JR. A step further in gas turbine dynamic simulation. Proceedings of the Institution of Mechanical Engineers, Part A: Journal of Power and Energy 2003;217(6):583–92.
[43] Kim J, et al. Model development and simulation of transient behavior of heavy duty gas turbines. J Eng Gas Turbines Power 2001;123(3):589–94.
[44] Rossi I, Traverso A, Tucker D. SOFC/Gas Turbine Hybrid System: A simplified framework for dynamic simulation. Appl Energy 2019;238:1543–50.
[45] Gimelli A, Sannino R. Thermodynamic model validation of Capstone C30 micro gas turbine. Energy Procedia 2017;126:955–62.
[46] Davison CR, Birk A. *Steady state and transient modeling of a micro-turbine with comparison to operating engine*. in *Turbo Expo: Power for Land*. Sea, and Air 2004.
[47] Davison CR, Birk A. *Comparison of transient modeling techniques for a micro turbine engine*. in *Turbo Expo: Power for Land*. Sea, and Air 2006.
[48] Kim S, Park J, Goldenberg VL. *Investigation of transient performance of an auxiliary power unit microturbine engine*. in *Turbo Expo: Power for Land*. Sea, and Air 2006.
[49] Hashmi MB, et al. Transient Behavior in Variable Geometry Industrial Gas Turbines: A Comprehensive Overview of Pertinent Modeling Techniques. Entropy 2021;23(2):250.
[50] Willenborg, K., et al. Experimental Studies of the Boundary Conditions Leading to Oil Fire in the Bearing Chamber and in the Secondary Air System of Aeroengines. in Turbo Expo: Power for Land, Sea, and Air. 2002.
[51] Verstraete, T., Z. Alsalihi, and R. Van den Braembussche, *Numerical study of the heat transfer in micro gas turbines*. 2007.
[52] Xiong J, et al. The additional control strategies to improve primary frequency response for hybrid power plant with gas turbines and steam turbines. Energy Rep 2022;8:557–64.
[53] Rowen WI. Simplified mathematical representations of heavy-duty gas turbines. Journal of engineering for power 1983;105(4):865–9.
[54] Rowen WI. Simplified mathematical representations of single shaft gas turbines in mechanical drive service. ASME 1992 International Gas Turbine and Aeroengine Congress and Exposition. American Society of Mechanical Engineers; 1992.
[55] Yang R, et al. Hybrid improved particle swarm optimization-cuckoo search optimized fuzzy PID controller for micro gas turbine. Energy Rep 2021;7: 5446–54.
[56] De Paepe W, et al. Control Strategy Development for Optimized Operational Flexibility From Humidified Micro Gas Turbine: Saturation Tower Performance Assessment. Turbo Expo: Power for Land, Sea, and Air. American Society of Mechanical Engineers; 2021.
[57] Yang J, et al. Thermodynamic modelling and real-time control strategies of solar micro gas turbine system with thermochemical energy storage. J Clean Prod 2021;304:127010.
[58] Zhang X, et al. Research on Modeling and Control of a 100 kW Micro Bio-Gas Turbine. Journal of Power and Energy Engineering 2021;9(02):1.
[59] Cameretti, M.C., et al. *An optimal control strategy for High-Speed Micro Gas Turbine Permanent-Magnet Synchronous Generator*. in *2018 International Symposium on Power Electronics, Electrical Drives, Automation and Motion (SPEEDAM)*. 2018. IEEE.
[60] Huang B, Qi Y, Murshed AM. Dynamic modeling and predictive control in solid oxide fuel cells: first principle and data-based approaches. John Wiley & Sons; 2013.
[61] Rossi I, Zaccaria V, Traverso A. Advanced Control for Clusters of SOFC/Gas Turbine Hybrid Systems. J Eng Gas Turbines Power 2018;140(5).
[62] Zaccaria V, Ferrari ML, Kyprianidis K. Adaptive Control of Microgas Turbine for Engine Degradation Compensation. J Eng Gas Turbines Power 2020;142(4).
[63] Zhu, M., et al. *Modeling and model predictive control of micro gas turbine-based combined cooling, heating and power system*. in *2016 Chinese Control and Decision Conference (CCDC)*. 2016. IEEE.
[64] Wu X, et al. Data-driven predictive control of micro gas turbine combined cooling heating and power system. IFAC-PapersOnLine 2016;49(27):419–24.
[65] Shixi M, et al. Micro Gas Turbine/Renewable Hybrid Power System for Distributed Generation: Effects of Ambient Conditions on Control Strategy. Turbo Expo: Power for Land, Sea, and Air. American Society of Mechanical Engineers; 2016.
[66] Moustafa I, Hassan M. Speed control of micro gas turbine with PMSG using evolutionary computational techniques. The International Conference on Electrical Engineering. Military Technical College; 2016.

[67] Alizadeh S, Sedighizadeh M, Arzaghi-Haris D. Optimization of micro-turbine generation control system using genetic algorithm. 2010 IEEE International Conference on Power and Energy. IEEE; 2010.
[68] Deng, W. and H. Zhang. *Fuzzy neural networks adaptive control of micro gas turbine with prediction model*. in *2006 IEEE International Conference on Networking, Sensing and Control*. 2006. IEEE.
[69] Wang, J., C. Zhang, and Y. Jing. *Adaptive PID control with BP neural network self-tuning in exhaust temperature of micro gas turbine*. in *2008 3rd IEEE conference on industrial electronics and applications*. 2008. IEEE.
[70] Wang, J.-J., C.-F. Zhang, and Y.-Y. Jing. *Self-adaptive RBF neural network PID control in exhaust temperature of micro gas turbine*. in *2008 International Conference on Machine Learning and Cybernetics*. 2008. IEEE.
[71] Wu B. Dynamic performance simulation analysis method of split shaft gas turbine based on RBF neural network. Energy Rep 2021;7:947–58.
[72] Lin P, et al. Modeling and controller design of a micro gas turbine for power generation. ISA Trans 2020.
[73] Wei, H., et al. *Dynamic modelling and simulation of a Micro-turbine generation system in the microgrid*. in *2008 IEEE International Conference on Sustainable Energy Technologies*. 2008. IEEE.
[74] Li, P., et al. *Modeling and control of a gas micro turbine generator by using a causal ordering graph*. in *The Proceedings of the Multiconference on" Computational Engineering in Systems Applications"*. 2006. IEEE.
[75] Mirandola S, et al. Modeling of a hybrid externally fired gas turbine applied to a landfill and green waste management facility. Energ Conver Manage 2021;244:114483.
[76] Al-Attab KA, Zainal Z. Externally fired gas turbine technology: A review. Appl Energy 2015;138:474–87.
[77] Camporeale SM, et al. Externally fired micro-gas turbine and organic rankine cycle bottoming cycle: Optimal biomass/natural gas combined heat and power generation configuration for residential energy demand. J Eng Gas Turbines Power 2017;139(4).
[78] Al-attab KA, Zainal Z. Turbine startup methods for externally fired micro gas turbine (EFMGT) system using biomass fuels. Appl Energy 2010;87(4):1336–41.
[79] Agostini A, et al. Environmental Impacts of a Solar Dish Coupled With a Micro-Gas Turbine for Power Generation. *Front* Energy Res 2021;9:776821.
[80] Cameretti MC. Modelling of a Hybrid Solar Micro-Gas Turbine fuelled by biomass from agriculture product. Energy Rep 2020;6:105–16.
[81] Semprini S, Sanchez D, De Pascale A. Performance analysis of a micro gas turbine and solar dish integrated system under different solar-only and hybrid operating conditions. Sol Energy 2016;132:279–93.
[82] Traverso A, et al. *Dynamic analysis of concentrated solar hybridised gas turbine*. Turbo Expo: Power for Land, Sea, and Air. American Society of Mechanical Engineers; 2014.
[83] Bashir MA, et al. Effect of Phase Change Materials on the short-term thermal storage in the solar receiver of dish-micro gas turbine systems: A numerical analysis. Appl Therm Eng 2021:117179.
[84] Tian Y, Zhao C-Y. A review of solar collectors and thermal energy storage in solar thermal applications. Appl Energy 2013;104:538–53.
[85] Ghavami M. Cycle analysis and optimisation of micro gas turbines for concentrated solar power. City: University of London; 2017.
[86] Felsmann C, Gampe U, Freimark M. *Dynamic behavior of a solar hybrid gas turbine system*. Turbo Expo: Power for Land, Sea, and Air. American Society of Mechanical Engineers; 2015.
[87] Kathirgamanathan D, Axelsson L-U. *Rotor over-speed analysis of a hybrid solar gas turbine*. Turbo Expo: Power for Land, Sea, and Air. American Society of Mechanical Engineers; 2018.
[88] Ghavami M, Alzaili J, Sayma A. A comparative study of the control strategies for pure concentrated solar power micro gas turbines. Turbo Expo: Power for Land, Sea, and Air. American Society of Mechanical Engineers; 2017.
[89] Barberis, S., et al. *High temperature storage for CSP plants: Test rig dynamic analysis*. in *Proceedings of 7th International Gas Turbine Conference, Brussels, Belgium*. 2014.
[90] Barberis S, et al. High Temperature Storage for CSP Hybrid Gas Turbine: Test Rig Dynamic Analysis and Experimental Validation. Turbo Expo: Power for Land, Sea, and Air. American Society of Mechanical Engineers; 2016.
[91] Mahmood M, et al. Thermal energy storage for CSP hybrid gas turbine systems: Dynamic modelling and experimental validation. Appl Energy 2018;212:1240–51.
[92] Chen J, et al. Dynamic simulation of a solar-hybrid microturbine system with experimental validation of main parts. Renew Energy 2020;154:187–200.
[93] Xu Z, et al. Experimental evaluation of 100 kW grade micro humid air turbine cycles converted from a microturbine. Energy 2019;175:687–93.
[94] Delattin F, et al. Effects of steam injection on microturbine efficiency and performance. Energy 2008;33(2):241–7.
[95] De Paepe W, et al. Toward higher micro gas turbine efficiency and flexibility—humidified micro gas turbines: a review. J Eng Gas Turbines Power 2018;140(8).
[96] Carrero MM, et al. Experimental characterisation of a micro Humid Air Turbine: assessment of the thermodynamic performance. Appl Therm Eng 2017;118:796–806.
[97] De Paepe W, et al. T100 micro Gas Turbine converted to full Humid Air Operation: Test rig evaluation. Turbo Expo: Power for Land, Sea, and Air. American Society of Mechanical Engineers; 2014.
[98] De Paepe W, et al. T100 micro gas turbine converted to full humid air operation: A thermodynamic performance analysis. Turbo Expo: Power for Land, Sea, and Air. American Society of Mechanical Engineers; 2015.
[99] Huang, D., et al. *Modeling and Simulation of Saturator Temperature Control in Humid Air Turbine Cycle*. in *ASME International Mechanical Engineering Congress and Exposition*. 2017. American Society of Mechanical Engineers.
[100] Williams MC, Strakey JP, Singhal SC. US distributed generation fuel cell program. J Power Sources 2004;131(1–2):79–85.
[101] Kwan TH, et al. Comprehensive review of integrating fuel cells to other energy systems for enhanced performance and enabling polygeneration. Renew Sustain Energy Rev 2020;128:109897.
[102] Azizi MA, Brouwer J. Progress in solid oxide fuel cell-gas turbine hybrid power systems: System design and analysis, transient operation, controls and optimization. Appl Energy 2018;215:237–89.
[103] Baudoin S, et al. Analysis and validation of a biogas hybrid SOFC/GT emulator. IEEE; 2014.
[104] Veyo SE, et al. *Status of pressurized SOFC/GAS turbine power system development at Siemens Westinghouse*. in *Turbo Expo: Power for Land*. Sea, and Air 2002.
[105] Miyamoto K, et al. Recent progress of SOFC combined cycle system with segmented-in-series tubular type cell stack at MHPS. ECS Trans 2015;68(1):51.
[106] Larosa, L., A. Traverso, and A.F. Massardo. *Dynamic analysis of a recuperated mGT cycle for fuel cell hybrid systems*. in *Turbo Expo: Power for Land, Sea, and Air*. 2016. American Society of Mechanical Engineers.
[107] Zhang X, et al. A review of integration strategies for solid oxide fuel cells. J Power Sources 2010;195(3):685–702.
[108] Chinda P, Brault P. The hybrid solid oxide fuel cell (SOFC) and gas turbine (GT) systems steady state modeling. Int J Hydrogen Energy 2012;37(11):9237–48.
[109] Buonomano A, et al. Hybrid solid oxide fuel cells–gas turbine systems for combined heat and power: a review. Appl Energy 2015;156:32–85.
[110] Komatsu Y, Kimijima S, Szmyd JS. Performance analysis for the part-load operation of a solid oxide fuel cell–micro gas turbine hybrid system. Energy 2010;35(2):982–8.
[111] Lv X, et al. Determination of safe operation zone for an intermediate-temperature solid oxide fuel cell and gas turbine hybrid system. Energy 2016;99:91–102.
[112] Kandepu R, et al. Modeling and control of a SOFC-GT-based autonomous power system. Energy 2007;32(4):406–17.
[113] McLarty DF. Fuel cell gas turbine hybrid design, control, and performance. Irvine: University of California; 2010.
[114] Steilen, M., *Thermodynamic modeling and experimental investigation of operating conditions for a SOFC/GT hybrid power plant.* 2019.
[115] Roberts RA. A dynamic fuel cell-gas turbine hybrid simulation methodology to establish control strategies and an improved balance of plant. Irvine: University of California; 2005.
[116] Brouwer, J., *Hybrid gas turbine fuel cell systems, Chapter 4*. 2006, AD Richard, The Gas Turbine Handbook, Morgantown, West Virginia: Department ….
[117] Larosa L, et al. Pressurized SOFC hybrid systems: control system study and experimental verification. J Eng Gas Turbines Power 2015;137(3).
[118] Ferrari ML, et al. Advanced control system for grid-connected SOFC hybrid plants: experimental verification in cyber-physical mode. J Eng Gas Turbines Power 2019;141(9).
[119] Zhang B, et al. Rapid load transition for integrated solid oxide fuel cell–Gas turbine (SOFC-GT) energy systems: A demonstration of the potential for grid response. Energ Conver Manage 2022;258:115544.
[120] Liese, E.A., et al. *Technical development issues and dynamic modeling of gas turbine and fuel cell hybrid systems*. in *Turbo Expo: Power for Land, Sea, and Air*. 1999. American Society of Mechanical Engineers.
[121] Birol, F., *The Future of Hydrogen (IEA)*. 2019, Paris.
[122] Goldmeer, J., *Power to gas: Hydrogen for power generation.* GEA33861, February, 2019.
[123] Banihabib R, Assadi M. A Hydrogen-Fueled Micro Gas Turbine Unit for Carbon-Free Heat and Power Generation. Sustainability 2022;14(20):13305.
[124] Zornek T, Monz T, Aigner M. Performance analysis of the micro gas turbine Turbec T100 with a new FLOX-combustion system for low calorific fuels. Appl Energy 2015;159:276–84.
[125] Nikpey H, Assadi M, Breuhaus P. Experimental investigation of the performance of a micro gas turbine fueled with mixtures of natural gas and biogas. American Society of Mechanical Engineers; 2013.
[126] de Santoli L, et al. Seasonal energy and environmental characterization of a micro gas turbine fueled with H2NG blends. Energy 2020;193:116678.
[127] Gholamian E, et al. Dynamic simulation and techno-economic assessment of hydrogen utilization in dual fuel (Hydrogen/biogas) micro gas turbine systems for a wastewater treatment plant. Process Saf Environ Prot 2022.
[128] Renzi M, Patuzzi F, Baratieri M. Syngas feed of micro gas turbines with steam injection: Effects on performance, combustion and pollutants formation. Appl Energy 2017;206:697–707.
[129] Reale F, Sannino R. Water and steam injection in micro gas turbine supplied by hydrogen enriched fuels: Numerical investigation and performance analysis. Int J Hydrogen Energy 2021.